AD-A079 125 MASSACHUSETTS UNIV AMHERST DEPT OF POLYMER SCIENCE --ETC F/G 13/8
SOLID STATE EXTRUSION OF NYLONS 11 AND 12; PROCESSING, MORPHOLO--ETC(U)
DEC 79 W G PERKINS , R S PORTER N00014-75-C-0686

UNCLASSIFIED TR-12 NL

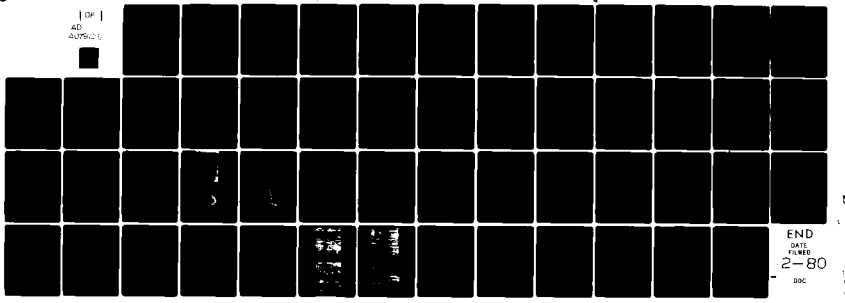

END
DATE FILMED
2-80
DDC

AD A079125

OFFICE OF NAVAL RESEARCH

Contract No. N00014-75-C-0686

Project No. NR 356-584

TECHNICAL REPORT NO. 12

"SOLID STATE EXTRUSION OF NYLONS 11 and 12; PROCESSING, MORPHOLOGY AND PROPERTIES"

by

William G. Perkins and Roger S. Porter
Polymer Science and Engineering Department
Materials Research Laboratory
University of Massachusetts
Amherst, Massachusetts 01003

DDC
JAN 10 1980
A

December 14, 1979

Reproduction in whole or in part is permitted for any purpose of the United States Government

Approved for Public Release; Distribution Unlimited

DDC FILE COPY

80 1- 9 049

ABSTRACT

Monofilaments of poly(11-amino-undecanoic acid) (nylon 11), and poly-(laurylactam) (nylon 12) have been produced via solid state extrusion in an Instron capillary rheometer. The resulting morphology plus physical and mechanical properties were investigated. For nylon 11, crystalline melting point (T_m) increase 16°C at an extrusion ratio (ER) of 12, over the undrawn material, while percent crystallinity (X_c) was up 23%. Nylon 12, extruded to a maximum ER of 6, realized an increase in T_m of 4°C at ER=5 and an X_c increase of 14%. Young's modulus for nylon 11 increased from 3GPa at an ER=3 to 5.5 GPa at an ER=7, then levelled off at higher draw. For nylon 12, the value climbed from 2.5 at ER=3 to ~3.3 GPa at ER=5.5. Conventionally melt-spun and cold-drawn nylon 11 fibers exhibit a Young's modulus of 2.7 GPa; nylon 12 fibers, 2.9 GPa. Atmospheric moisture loss was found not to affect solid state extrusion of these higher nylons. Increases in extrusion temperature and/or pressure increased extrusion rate. The flow activation energy of nylon 11 was 73 Kcal/mole at 0.24 GPa extrusion pressure, and 124 Kcal/mole at 0.49 GPa. Calculated apparent viscosities were $\sim 10^{14}$ poise and $\sim 10^{15}$ poise respectively. The morphologies were shown by electron microscopy to be microfibrillar and the resulting monofilaments were transparent to visible light.

DTIC

INTRODUCTION

Solid state extrusion of high density polyethylene has provided films and fibers of exceptionally high modulus and tensile strength (1,2). It was thought that studies with the hydrogen-bonded nylons would expand the state-of-the-art of crystalline-state extrusion into polymers with higher melting points. The higher nylons were chosen for initial studies because of their longer olefinic segments.

This study involves the process-structure-property relationships of nylon 11 [poly(11-amino-undecanoic acid)] and nylon 12 [poly(laurylactam)] extruded in the crystalline state. Discussion of results is divided into parts on nylon 11 and on nylon 12.

EXPERIMENTAL

Solid state extruded nylon morphologies were prepared in an Instron capillary rheometer by the technique detailed previously (3). Variations on the process included crystallization and extrusion at several temperatures and pressures, as well as extrusion at constant rates (fixed crosshead speed) up to a predetermined maximum pressure. When the maximum pressure was attained, the load was cycled between narrow limits to maintain near constant pressure.

Differential scanning calorimetry (DSC) was performed on the starting nylons and extrudates with a Perkin-Elmer DSC-1B at a heating rate of $10^{o}C\text{-}min^{-1}$ to yield heats of fusion (converted to percent crystallinity, X_c) and crystalline melting points, T_m. Entropy of fusion was calculated from the above parameters through their thermodynamic relationship.

A Perkin-Elmer TMS-1 thermomechanical analyzer attachment to the DSC-1B was used for measurement of the linear expansion coefficient, α. Sample preparation for this test was as previously described (4). A load of 3 grams was used with the expansion probe, and the scanning rate was $10^{o}C\text{-}min^{-1}$. Test sample length was approximately 1 cm. Scans were made from $-140^{o}C$ up to $190^{o}C$.

For studies of fiber mechanical properties, an Instron tensile testing machine, model TTCM, equipped with a 10 mm strain-gauge extensometer, was used. Load-elongation curves were obtained at room temperature using a fixed elongation rate of 0.02 $cm\text{-}min^{-1}$ for modulus measurements and 0.50 $cm\text{-}min^{-1}$ for determination of tensile strength and strain at break. Samples were gripped

in special clamps described elsewhere (1) to prevent slippage in the jaws. Nevertheless, slippage occurred during testing of nylon 11 ultimate properties, rendering impossible determination of tensile strength and strain at break. Strain rates for determination of Young's modulus and tensile strength (nylon 12) were 3.33×10^{-4} sec^{-1} and 1.67×10^{-3} sec^{-1}, respectively. The Young's modulus was determined as the tangent to the stress-strain curve at 0.2% strain.

Dilute solution viscosity measurements were conducted in a silicone oil bath using a #100 Ubbelohde viscometer. The solvent was m-cresol and test temperature was $50^{o}C$. Efflux time for the solvent was ~ 300 sec.

Part I - Nylon 11

Introduction

The nylon 11 used was supplied by the Rilsan Corporation, Glen Rock, New Jersey, having a reported $\overline{M_w}$ = 34,000 and $\overline{M_n}$ = 13,000. The crystalline melting point of the as-received material was $189^{o}C$ and the heat of fusion, 11.26 $cal\text{-}gm^{-1}$. This corresponds to ~ 21% crystallinity, as the heat of fusion for 100% crystalline nylon 11 has been calculated to be 53 $cal\text{-}gm^{-1}$ (5,6).

The principal crystal structure of nylon 11 has been investigated (7-9) and found to exist in a planar zigzag conformation. The unit cell contains one monomer unit and is triclinic, having dimensions a = 4.9Å, b = 5.4Å, c (chain axis) = 14.9Å; $\alpha = 49^{o}$, $\beta = 77^{o}$, $\gamma = 63^{o}$ (7). Polymorphism exists in nylon 11 as it does in virtually all the polyamides.

Above 70°C, Genas (8) found that the a,b (basal) plane of the triclinic cell assumes pseudohexagonal packing. Onogi, et. al (9) observed that quenched film of nylon 11 contains γ (pseudohexagonal) crystals, whereas film solution-cast from m-cresol contains α (triclinic) crystals. When films containing γ crystals were annealed above 90°C, they transformed into the α modification. This $\gamma \rightarrow \alpha$ transformation can also occur on stretching (10).

Figure 1a is a wide angle x-ray photograph of a nylon 11 extrudate solid state extruded to an extrusion draw ratio of 7. The diffraction pattern is consistent with that for the α (triclinic) modification. It has been suggested (11) that the "parallel" structure of nylon 11, wherein the polar amide groups are tilted with respect to the chain axes, represents a stronger hydrogen bond association than does the "antiparallel" modification. This is consistent with the triclinic unit cell generally observed at room temperature (7-9). The parallel modification arises when neighboring chains lie all in the same direction. In the antiparallel form, the chains alternate in direction. There is a difference between the two forms because the sequence of chain atoms encountered in going along the chain in one direction for ω-amino acid polyamides is the reverse of that found in traveling in the opposite direction (12). For the odd ω-amino acid nylons such as nylon 11, both the parallel and anti-parallel forms allow complete hydrogen bonding (7,13). Such is not the case for the even ω-amino acid nylons (e.g. nylon 12), discussed in Part II.

The effects of pressure on the crystallization and structure of nylon 11 have been reported (14,15). Gogolewski and Pennings (14) found that pressures exceeding 3 Kbar (0.29 GPa) and temperatures higher than 230°C are sufficient for growth of chain-extended crystals, either by pressure-induced crystallization from the melt or by annealing of the folded chain crystals. They note that the α (triclinic) crystalline modification, commonly found for folded chain crystals of nylon 11, was preserved in the high pressure crystallization and annealing experiments. They concluded that during the initial stages of crystallization under pressure, folded chain crystals are formed, with a crystalline order and long spacing larger than that of the starting nylon 11. These authors noted a 16°C/Kbar melting point increase with pressure.

Newman, et al. (15), performed a detailed x-ray structure analysis on nylon 11 at various temperatures and pressures. They concluded that the chain conformation of Slichter (7) was distorted (shortened) along the c-axis at ambient temperature and pressure. No phase transformations from the α crystal structure were observed at room temperature up to pressures of 19.5 Kbar (1.9 GPa). However, a crystal transition at atmospheric pressure was observed at 95°C, the triclinic (α phase) changing to a pseudohexagonal structure. It was found that the increase in transition temperature with pressure was ~ 15°C/Kbar.

DTA measurements by Gordon (16) show that the commonly observed glass transition at 43°C disappears if a sample is annealed at 75°C for 24 hours.

A transition appears instead at 92°C. However, after 3 days at room temperature, samples show transitions at both 40 and 92°C. He concludes that the type of hydrogen bonded network formed from the melt depends on the temperature of formation and the break-up of such networks is responsible for observed glass transitions. He postulates that the network formed at the (ambient) annealing temperature is relatively stable, but the continuing motion of the paraffinic segments leads to generation of another network.

Further work on transitions in nylon 11 was reported by Northolt, et al. (17). Results from DSC, tensile testing and wide angle x-ray measurements on oriented samples aged at various temperatures revealed that the glass transition in nylon 11 shifted to higher temperatures as samples were aged at progressively higher temperatures. This was seen as resulting from amorphous phase hydrogen bond weakening at the higher (aging) temperatures and their subsequent orientation and reformation. No effect of moisture on transitions was reported.

The presence of several relaxations in nylon 11 has been observed by Onogi, et al. (9) in dynamic mechanical spectra. They suggest that the primary, ie. glass transition, relaxation is at ~ 70°C with a smaller relaxation at -50°C. Another relaxation is seen at ~ +160°C. This dispersion may be analogous to the α transition in polyethylene at from 80 - 100°C (18).

Experimental Results

The effect of extrusion temperature and pressure on extrusion rate is shown in Figure 2. This is a plot of extrudate length vs. extrusion time at two temperatures and pressures. Extrusion pressure in the lower time curves is 0.24 GPa (2400 atm). As expected, the higher extrusion temperature results in an initially higher extrusion rate. However, both extrusion rates reduce with time and essentially stop. The upper curves in Figure 2 show the effect of extrusion temperature on extrusion rate at a (maximum) extrusion pressure of 0.49 GPa (5000 atm). Although the initial extrusion rate is also slightly higher at higher extrusion temperature, at long times the two (extrudate length vs. extrusion time) curves diverge whereas at the lower pressure the two curves converge. Also at the higher pressure, the curves at both extrusion temperatures do not tend to zero at long times, although their slopes are decreasing.

Table 1 shows the results of dilute solution viscosity measurements on both virgin nylon 11 pellets and on fibers extruded at several temperatures. The lack of viscosity change with time, at any extrusion temperature, indicates that the polymer did not undergo degradation during extrusion.

The effect of moisture content on the extrusion rate of nylon 11 is shown in Figure 3. One sample (circles) was dried in a vacuum oven at 100°C for 24 hours then stored in a desiccator over P_2O_5 under vacuum. The triangles represent data for nylon 11 which had no conditioning prior to processing. All points fall on the same curve indicating negligible effect of adsorbed water

on extrusion rate. A third sample was immersed in steam at atmospheric pressure for 71 hours. Upon removal of the restrictor at the beginning of extrusion, the extrusion pressure immediately dropped toward zero and a foamed melt rapidly extruded.

The effect of pulling on the emerging extrudate is shown in Figure 4. Nylon 11 was extruded at 0.49 GPa and 194^{o}C and a 5 kg weight was attached to the extrudate. The initial extrusion rate was somewhat faster than under the same conditions but without attached weights. However, at long times no significant increase in extrusion rate was observed on pulling.

Figures 5 - 7 illustrate several physical properties of solid state extruded nylon 11 and their relationship to extrusion (draw) ratio (ER). Figure 5 shows a rise in T_m with ER to about 205^{o}C at an ER of 12. This represents a 16^{o}C increase over the undrawn virgin material (ER = 1). Percent crystallinity (X_c) as measured by DSC vs. ER is shown in Figure 6. Crystalline content also increases significantly with ER from ~ 21% to ~ 44% at an ER of 10. At ER = 12, the lower values may be experimental error. Figure 7 shows that the entropy of fusion (ΔS_f) rises steeply to ER = 3 and then approaches a limit.

Figure 8 is a plot of Young's modulus vs. ER. The maximum value attained was ~ 5.5 GPa, obtained at an ER of 7, remaining constant thereafter. This compares to a Young's modulus of 1.3 GPa exhibited by injection molded parts, and 2.7 GPa obtained from commercially spun and drawn filaments.

Part II - Nylon 12

Introduction

The nylon 12 used in this study was supplied by Dr. Akiro Kishimoto of the Toyo Seikan Company, Limited, Yokohama, Japan, having a reported $\overline{M_w} \tilde{=} 28,600$ and a $\overline{M_n} = 14,300$. The crystalline melting point of the as-received material was 179°C and a heat of fusion of 10.0 cal/gm corresponding to 18.5% crystallinity for a heat of fusion of 100% crystalline nylon 12 reported to be 54 cal/gm (6).

The crystal structure of nylon 12 has been found (19,20) to be a γ modification wherein the chains are twisted about the methylene groups. The conformation is planar zigzag. Inoue and Hoshino (20) prepared a sample by drawing a monofilament 3.6X in boiling water then annealing it at 160°C for 10 hours. They found a monoclinic unit cell resembling the γ-form of the other even nylons. From x-ray data they calculated the monoclinic unit cell dimensions as $a = 9.38\text{Å}$, $b = 32.2\text{Å}$ (fiber axis), $c = 4.87\text{Å}$ and $\beta = 121.5°$. There are four repeat monomer units per unit cell. Northolt, et al. (19), found that nylon 12 may exist in two different forms. Melt-pressed sheet, quenched in ice water, drawn 4.5X at room temperature, and annealed at 170°C at constant length for several hours under nitrogen, revealed a hexagonal unit cell. Melt-pressed sheet, quenched in ice water, drawn 7X at just under 180°C, and cooled under stress to room temperature, exhibited what appeared to be a mixture of mono- and triclinic unit cell structures. No transition to the α-form,

wherein chains are antiparallel, is observed for nylon 12 upon stretching or treatment with aqueous phenol. It was therefore concluded that the γ-form of nylon 12 is more stable than for nylon 6, nylon 8 or nylon 10. This led to the conclusion that the longer the molecular chain in the even nylons, the more the crystal shows a tendency to form the γ-phase (20,21). Nylon 12 is is always found in the "parallel" modification (13) wherein neighboring chains are all in the same direction. Because this would result in 50% free NH groups, a twisting of the molecule is necessary for the observed complete hydrogen bond formation. This twisting causes a shortening of the unit cell along the chain (b) axis and results in the γ-form of the crystal. The wide angle x-ray diffraction pattern shown in Figure 1b is a typical pattern for the γ-phase of the even nylons. The strong intensity of the meridional diffraction spots results from the carbonyl oxygen atoms all lying in planes perpendicular to the fiber axis (21).

Crystallization and annealing under high pressure (4.9 Kbar - 0.48 GPa) was carried out by Stamhuis and Pennings (26). They noted that a partial transformation of the pseudo-hexagonal or monoclinic γ-crystal structure to an α modification occurred in samples crystallized at 240°C and 4.9 Kbar for 16 hours. In the pressure range up to 3 Kbar (0.29 GPa) the increase in melting temperature was ~ 20°C/Kbar, whereas at a pressure of 8 Kbar (0.78 GPa), the relationship was found to be 12°C/Kbar. The authors observed no chain-extended crystals, although a broadening of the distribution of crystal dimensions was noted at the higher crystallization pressures.

Onogi, et al. (9), found no evidence of an α-type relaxation for nylon 12 (as for polyethylene) by dynamic mechanical tests, as they did for nylon 11 at ~ 160°C.

Results

The effect of extrusion temperature on extrusion rate is shown in Figure 9. The initial rate is higher at the higher temperature but after 15 minutes the rates are both slower and equivalent. At longer extrusion times, the lower temperature extrusion rate begins to level off, while the higher temperature extrusion rate continues to increase, albeit more slowly than at short times.

Figure 10 shows the effect of crystallization/extrusion pressure on crystalline melting point (T_m) and percent crystallinity (X_c) of solid state extruded nylon 12. Crystallization and extrusion pressures were equal and as shown in this figure, T_m decreases linearly with extrusion pressure from 0.12 to 0.24 GPa, then remains constant, whereas percent crystallinity rises steadily with extrusion pressure to 0.24 GPa before levelling off.

The influence of crystallization/extrusion temperature on the crystalline melting point and crystallinity for nylon 12 fibers is shown in Figure 11. The crystallization and extrusion temperatures were equal, and as shown, the melting point increased about 3°C as crystallization/extrusion temperature was increased from 176 to 196°C. The crystallinity rises from ~ 19% to ~ 30% for an increase in crystallization/extrusion temperature of 8°C, then levels off at higher preparation and extrusion temperatures.

Figure 12 shows an increase in T_m from 179°C for undrawn material (ER = 1) to 183°C for fibers extruded to an ER of ~ 5, whereas the crystallinity increased from 19% from undrawn to 33% for extrudates drawn to about 6X. Both curves indicate significant increases in crystalline perfection with increasing ER.

Figure 13 shows that the entropy of fusion (ΔS_f) exhibits an initial sharp increase with ER followed by a more gradual increase at higher values.

Thermomechanical analyses were performed on nylon 12 fiber at an extrusion ratio of 5 (Figure 14). This is a semi-logarithmic plot of the normalized change in length of the fiber, i.e. orientation direction, vs. scanning temperature. The upper curve is for a melt extruded (disoriented) fiber whereas the bottom curve depicts the behavior of a solid state extruded fiber (ER = 5) of the same nylon 12. The melt extruded fiber has a large positive expansion coefficient (slope of the curve) up to the melting point of 179°C. The solid state extruded fiber has a smaller positive expansion coefficient up to -70°C, then contracts rapidly on further heating. Results of temperature cycling in the TMA experiment are shown in Figure 15 and are discussed in the next section.

Figure 16 shows the change in Young's modulus with ER. For an increase in extrusion ratio from 3 to 5.5, the tensile modulus gradually increases from 2.6 to 3.3 GPa. Mechanical data are compared in Table 2 for molded, commercially melt-spun and cold-drawn, and solid state extruded (ER = 5.5) samples.

DISCUSSION AND CONCLUSIONS

Several factors come into play during the solid state extrusion of nylon. As with other polymers, strain hardening (defined below) plays an important role, as does molecular weight and conditions for preparation of morphology prior to extrusion. Nylon extrusion is also affected by the hydrogen bonding of amide groups between chains. These bonds have a dissociation energy of ~ 8 Kcal/mole and serve to tie nylon molecules together. They exist in the noncrystalline as well as crystalline regions of nylons (23).

The influence of intermolecular hydrogen bonding on the flow of polymer melts has been investigated (24) with copolymers of ethylene and acrylic and methacrylic acids. An interesting result is that an increase in the amount of hydrogen bonding substantially enhances both flow activation energy and viscosity. In this sense, the lower nylons, such as -66 and -6, may be difficult to solid state extrude because of their abundant hydrogen bonding which inhibits sliding displacement along consecutive hydrogen bonded planes, a common deformation mode (25).

The effect of pressure on hydrogen bonding has not been widely investigated but there is evidence (26) that increasing pressure causes a decrease in the distance between the planes containing the hydrogen bonds as well as between the planes held by van der Waals interactions. This compressed structure would also likely retard flow in solid state extrusion.

Flow activation energies (E_a) were calculated for nylon 11 in this study at two extrusion pressures using the equation

$$\frac{d(\ln \eta)}{d\,(1/T)} = \frac{E_a}{R} \qquad (1)$$

where T = extrusion temperature (K); R = gas law constant; η = apparent viscosity, calculated from

$$\eta = \frac{\sigma}{\frac{dL}{dt} \cdot \frac{1}{L}} \qquad (2)$$

where σ = shear (applied stress); $\frac{dL}{dt}$ = shear rate; L = length of extrudate where calculations were made.

The (apparent) activation energy doubled (73 to 124 Kcal/mole) with a doubling of extrusion pressure (0.24 to 0.49 GPa). Apparent viscosities during extrusion were calculated as ~ 10^{14} poise at 0.24 GPa extrusion pressure and ~ 10^{15} poise at 0.49 GPa, both measured at 190°C. High density polyethylene extruded in the solid state exhibits an apparent viscosity of 10^{12} - 10^{13} poise. Mead and Porter (27) found the flow activation energy of a high density polyethylene to be between 20 and 60 Kcal/mole when the polymer was solid state extruded at temperatures in the vicinity of the ambient melting point. Measurements were made at 0.24 GPa where the corresponding nylon 11 value was 73 Kcal/mole.

Nylon 11 exhibits a transition at 160°C whereas nylon 12 shows no such high temperature transition as detected by dynamic mechanical testing (9).

This (α) transition may well be responsible for the achievement of higher extrusion ratios and faster extrusion rates with nylon 11. Such relaxations are widely reported for other semicrystalline polymers, including polyethylene. They are generally believed to result from the onset of motions within the crystalline phase. Hashimoto, et al. (28), believe that the α transition in polyethylene results from orientation dispersion of crystallites accompanied by shearing of mosaic crystallites within the lamellae, and from molecular motion within the crystals. Other investigators have postulated kink (29,30) or twist (31) crystal defect motions, and chain rotation (32-34) as responsible for the observed α relaxation in polyethylene. These processes may actually occur in nylon 12 but be undetectable by dynamic mechanical testing due to their small magnitude (33). In any case, such motions in the crystalline phase should aid the extrusion process by imparting mobility.

Strain Hardening

Strain hardening is a phenomenon which is commonly observed on drawing semicrystalline polymers below their T_m, and usually somewhat below T_g for amorphous polymers. During strain hardening the molecules become oriented parallel to the deformation direction. For semicrystalline polymers such as the nylons, the original crystal lamellae are broken up during deformation and aligned in the orientation direction to form microfibrils (35,36). Figures 17 and 18 are scanning electron microscope (SEM) photographs of solid

state extruded nylon 12 extrudates fractured along the draw direction. Microfibrils can plainly be seen at each magnification. A result of this fibrillar (non-spherulitic) morphology wherein crystals are fairly uniform in size and perfection is shown in Figure 19. This depicts two extruded nylon 12 fibers photographed over print. The top fiber was melt extruded and is spherulitic and opaque, whereas the bottom fiber was extruded in the crystalline state and is transparent.

With the high nominal-extrusion-ratio dies commonly used in this laboratory, extrusion ratio (ER) of the extrudate increases with extrudate length. In the case of high density polyethylene, maximum attainable ER is limited by a fracture mechanism at extrusion ratios $\geq$ 40. The nylons investigated in this study also exhibited limiting extrusion ratios. Nylon 12 exhibited a maximum ER of ~ 7, and nylon 11 at ~ 12. In most cases, however, maximum ER were limited not by fracture of the extrudate, as is the case with polyethylene, but rather by the virtual cessation of extrusion. In other words, at long times (> 8 hours), extrusion rates for the nylons declined to < 1 mm/hr. Strain hardening of these polymers apparently reaches the point where even 0.49 GPa is insufficient pressure to force them through the die.

Pressure

The effect of crystallization pressure on nylons 11 and 12 has been investigated (14,22). The pressure range used in the present study for nylon 12 is below the pressure necessary for growth of extended chain crystals. The results presented here for nylon 12 indicate that, for the pressure range investigated, increasing crystallization/extrusion pressure causes the forma-

tion of a greater amount of crystals, but that these crystals are smaller in size and/or perfection. One would expect such increases since the undercooling is less at higher crystallization temperatures at a given pressure. The results may differ for conditions where pressure can produce extended-chain crystals (22).

MELTING BEHAVIOR

Both melting point and heat of fusion (here converted to percent crystallinity) are related to the entropy of fusion by

$$\Delta G_f = \Delta H_f - T_m \Delta S_f \qquad (3)$$

where ΔG_f = Gibbs free energy of fusion; ΔH_f = enthalpy (heat) of fusion; T_m = melting temperature in degrees Kelvin; ΔS_f = entropy of fusion. Tonelli (37) divides the entropy of fusion into two components, a constant volume contribution and a volume expansion contribution.

In the present study, the crystalline melting point increases more rapidly than the percent crystallinity. This may result from the small increase in entropy of fusion plotted against extrusion ratio in Figures 7 (nylon 11) and 13 (nylon 12) along with the relationship given in Equation (3). Such entropy behavior is expected from Tonelli's conclusions since both nylon 11 and 12 are known to exhibit polymorphism at elevated temperatures and/or under conditions of solid state deformation (7,8,15,16,19).

THERMOMECHANICAL ANALYSIS

Thermomechanical analysis (TMA) can be used as a qualitative measure of chain orientation and extension for measurements along the fiber direction.

Solid state extruded nylon 12 samples all showed an initial positive expansion coefficient that was smaller than the corresponding melt extruded sample (Figure 14). As the scanning temperature was increased, solid state extruded fibers irreversibly contracted in all cases at < $0^{o}C$. The initial small positive coefficient of expansion is due to orientation and possibly a small component of extended chain crystals which counteract the large positive coefficient arising from unoriented amorphous and folded-chain regions (38).

A solid state extruded sample of nylon 12 was heated from $-130^{o}C$ to $150^{o}C$ in the thermomechanical analyzer and then cooled again to $-130^{o}C$ followed by another heating cycle. The behavior on initial heating was as just described. However, upon recooling, the sample at first expanded (in the axial direction), then reached a constant length which did not vary (with cooling and reheating) from $-25^{o}C$ on the cooling cycle to ~ $0^{o}C$ on heating cycle (see Figure 15). Beyond this point, the sample shortened with increase in temperature up to the melting point as reported earlier for solid state extruded nylon 12. The plateau in Figure 15 apparently results from annealing of the morphology during the first heating cycle wherein hydrogen bonds are given sufficient mobility. The new structure is more stable and retains its dimensional stability up to ~ $0^{o}C$ above which instability occurs. In the temperature range $0 \rightarrow 150^{o}C$ (during heating), the fiber behaves the same before and after thermal treatment. This state likely consists of unoriented amorphous and crystalline regions stabilized by hydrogen bonds, along with an oriented and possibly an extended chain component which survives thermal annealing (at least up to $150^{o}C$).

MODULUS

Young's modulus of nylon 11 increases more rapidly with draw than nylon 12. However, beyond an ER of 7, the nylon 11 modulus remains constant. Because the tensile modulus of high density polyethylene begins to sharply increase only at extrusion ratios greater than 10, the nylons' potentially high mechanical properties may be realized only when higher ER's are attained. At any rate, nylon 11 fibers cold extruded in this study at an ER of 7 show an 80% increase in tensile modulus over commercial monofilaments. Nylon 12 fibers at an ER of 5.5 display a modulus equal to commercial monofilament.

In conclusion, the nylons appear to offer the promise of highly improved physical and mechanical properties if higher extrusion ratios can be realized. By the incorporation of certain additives prior to crystallization and extrusion, this may be possible. Another route may be the split billet technique recently developed in this laboratory (39). In the present study, mechanical tensile modulus was equal to or greater than that reported in the literature for these polymers. The melting point and crystallinity were significantly increased over virgin material. Further work on nylon systems is warranted.

REFERENCES

1. N.J. Capiati and R.S. Porter, J. Polym. Sci., Polym. Phys. Ed. 13, 1177 (1975).
2. W.G. Perkins, N.J. Capiati and R.S. Porter, Polym. Eng. Sci. 16, 200 (1976).
3. N.J. Capiati, S. Kojima, W.G. Perkins and R.S. Porter, J. Mater. Sci. 12, 334 (1977).
4. R.S. Porter, N.E. Weeks, N.J. Capiati and R.J. Krzewki, J. Therm. Anal. 8, 547 (1975).
5. M. Inoue, J. Polym. Sci., A-1, 3427 (1963).
6. R. Greco and L. Nicolais, Polymer 17, 1049 (1976).
7. W.P. Slichter, J. Polym. Sci. 36, 259 (1959).
8. M. Genas, Angew. Chem. 74, 535 (1962).
9. S. Onogi, K. Asada, Y. Fukui and I. Tachinaka, Bull. Inst. Chem. Res. Kyoto Univ. 52, 368 (1974).
10. T. Sasaki, J. Polym. Sci., B-3, 557 (1965).
11. W.O. Baker and C.S. Fuller, J. Am. Chem. Soc. 64, 2399 (1942).
12. R. Hill and E.E. Walker, J. Polym. Sci. 3, 609 (1948).
13. F.W. Lord, Polymer 15, 42 (1974).
14. S. Gogolewski and A.J. Pennings, Polymer 18, 660 (1977).
15. B.A. Newman, T.P. Sham and K.D. Pae, J. Appl. Phys. 48, 4092 (1977).
16. G.A. Gordon, J. Polym. Sci., A-2, 9, 1693 (1971).
17. M.G. Northolt, B.J. Tabor and J.J. van Aartsen, Progr. Colloid and Polym. Sci. 57, 225 (1975).

18. R. Boyd, A.C.S. Organic Coatings and Plastics Preprint 35 (2), 216 (1975).

19. M.G. Northolt, B.J. Tabor and J.J. van Aartsen, J. Polym. Sci., A-2, 10, 191 (1972).

20. K. Inoue and S. Hoshino, J. Polym. Sci., Polym. Phys. Ed. 2, 1077 (1973).

21. D.C. Vogelsong, J. Polym. Sci., A-1, 1055 (1963).

22. J.E. Stamhuis and A.J. Pennings, Polymer 18, 667 (1977).

23. C.G. Cannon, Spectrochim. Acta 16, 302 (1960).

24. L.L. Blyler and T.W. Haas, J. Appl. Polym. Sci. 13, 2721 (1969).

25. J.J. Point, M. Dosiere, M. Gillot and A. Goffin-Gerin, J. Mater. Sci. 6, 479 (1971).

26. S. Gogolewski and A.J. Pennings, Polymer 18, 650 (1977).

27. W.T. Mead and R.S. Porter, J. Polym. Sci., Polym. Sci. Symp., 63, 289 (1978).

28. T. Hashimoto, N. Yasuda, S. Suehiro, S. Nomura and H. Kawai, A.C.S. Polymer Preprints 17 (2), 118 (1976).

29. W. Pechold, S. Blasenbrey and S. Woerner, Kolloid Z. 189, 14 (1963).

30. P.E. McMahon, R.L. McCullough and A.A. Schlegel, J. Appl. Phys. 38, 4123 (1967).

31. D.H. Reneker, J. Polym. Sci. 59, 539 (1962).

32. J.D. Hoffman, G. Williams and E. Passaglia, J. Polym. Sci., C-14, 173 (1976).

33. C.A.F. Tuijnman, Polymer 4, 259 (1963).

34. R.L. McCullough, J. Macromol. Sci.-Phys. 9, 97 (1974).

35. A. Peterlin, J. Mater. Sci. 6, 490 (1971).

36. R.E. Robertson, J. Polym. Sci., Polym. Phys. Ed. 10, 2437 (1972).

37. A.E. Tonelli in "Analytical Calorimetry," R.S. Porter and J.F. Johnson, eds., Vol. 3, Plenum Press, New York, 1974.

38. D.W. Van Krevelen and P.J. Hoftyzer, "Properties of Polymers," Elsevier, Amsterdam, 1976, Chapter 4.

39. P.D. Griswold, A.E. Zachariades and R.S. Porter, to be published.

TABLE 1

Relative Viscosities of Nylon 11 Fibers Extruded at Temperatures Shown and Dissolved in m-Cresol at 50°C.

[conc. = .137 g/dL]

Extrusion Temperature °C	Relative Viscosity
Virgin Pellets	1.14
186	1.16
190	1.21
194	1.13
198	1.23

TABLE 2

Comparison of Mechanical Properties of Molded, Commercially Melt Extruded/Cold-Drawn, and Solid State (Cold) Extruded Nylon 12. The Latter at An Extrusion Ratio of 5.5 and $\bar{M}_w$ = 28,600 $\bar{M}_n$ = 14,300

Property	Molded *	Cold-Drawn †	Cold-Extruded
Tensile Modulus (GPa)	1.24	2.9	3.3
Tensile Strength (GPa)	.06	.31	.26
Elongation at Break (%)	300	40	38

*Modern Plastics Encyclopedia, 1976-77, Vol. 53, No. 10A, pg. 465.

†"Polymer Science & Materials", A.V. Tobolsky and H.F. Mark, eds., Interscience, New York, (1971) pg. 245.

CAPTIONS FOR FIGURES

1. Wide angle x-ray photographs of (a) nylon 12 and (b) nylon 11 solid state extruded fibers. Fiber axis vertical.
2. Extrudate length vs. extrusion time for nylon 11 fibers crystallized and extruded at 0.24 GPa (lower curves) and 0.49 GPa pressures and at temperatures shown.
3. Extrudate length vs. extrusion time for nylon 11 fiber both vacuum dried and non-dried prior to processing. Crystallized at 194°C and 0.24 GPa; extruded at 194°C and 0.49 GPa.
4. Extrudate length vs. extrusion time for a nylon 11 fiber without pulling (triangles) and with a 5 kg weight attached to the emerging extrudate (circles). Crystallized at 194°C and 0.24 GPa; extruded at 194°C and 0.49 GPa.
5. Crystalline melting point vs. extrusion ratio (ER) for a nylon 11 fiber crystallized at 194°C and 0.24 GPa; extruded at 194°C and 0.49 GPa. ER = 1 is undrawn material.
6. Percent crystallinity vs. ER for a nylon 11 fiber crystallized at 194°C and 0.24 GPa; extruded at 194°C and 0.49 GPa. ER = 1 is undrawn material.
7. Entropy of fusion vs. ER for a nylon 11 fiber crystallized at 194°C and 0.24 GPa; extruded at 194°C and 0.49 GPa. ER = 1 is undrawn material.
8. Young's modulus vs. ER for a nylon 11 fiber crystallized at 194°C and 0.24 GPa; extruded at 194°C and 0.49 GPa.
9. Extrudate length vs. extrusion time for nylon 12 fibers crystallized at 184°C and 0.24 GPa; extruded at 0.49 GPa and at temperatures shown.

10. Crystalline melting point and percent crystallinity vs. crystallization/extrusion pressure for nylon 12 fibers. Crystallization/extrusion temperature: 178°C. Measurements taken at an ER = 4.

11. Crystalline melting point and percent crystallinity vs. crystallization/extrusion temperature for nylon 12 fibers. Crystallization/extrusion pressure: 0.24 GPa. Measurements taken at an ER = 4.

12. Crystalline melting point and percent crystallinity vs. ER for nylon 12 fibers crystallized and extruded at 178°C and 0.24 GPa. ER = 1 is undrawn material.

13. Entropy of fusion vs. ER for nylon 12 fibers crystallized and extruded at 178°C and 0.24 GPa. ER = 1 is undrawn material.

14. Linear expansion coefficients (slopes) of melt extruded and solid state extruded (ER = 5) nylon 12 fibers. Solid state extruded fiber crystallized at 186°C and 0.24 GPa; extruded at 176°C and 0.49 GPa.

15. Temperature cycling of a nylon 12 fiber in the thermomechanical analyzer. Three cycles shown: heating, cooling and reheating. Slope of the plot is the linear expansion coefficient.

16. Young's modulus vs. ER for a nylon 12 fiber crystallized at 184°C and 0.24 GPa and extruded at 182°C and 0.49 GPa.

17. SEM photographs of solid state extruded nylon 12 fibers fractured (peeled) under liquid nitrogen along draw direction which is horizontal. ER = 7.

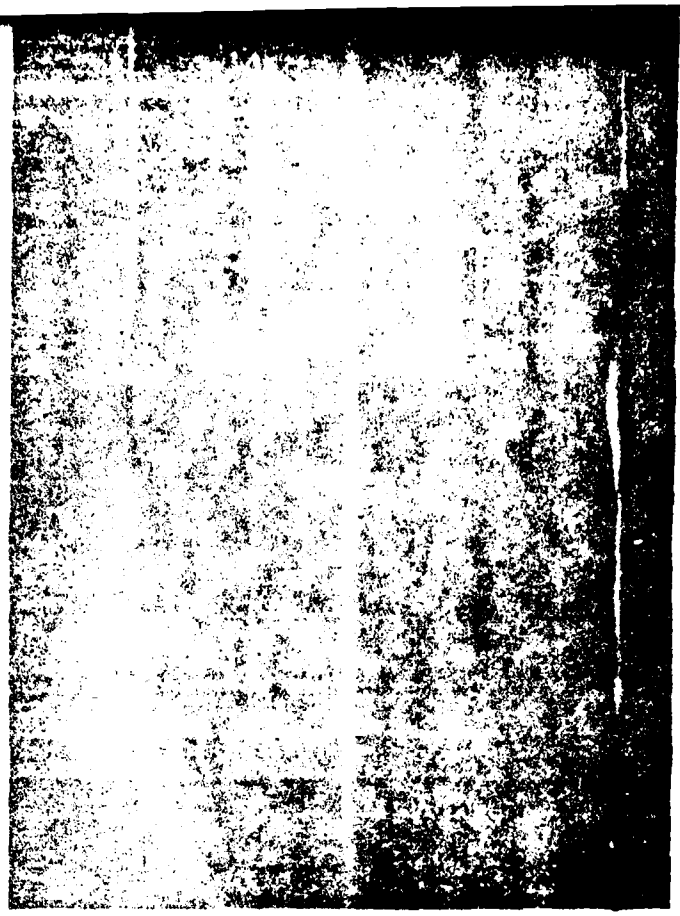

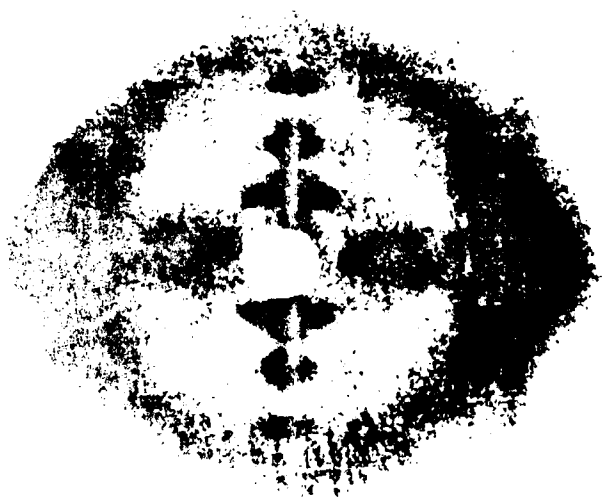

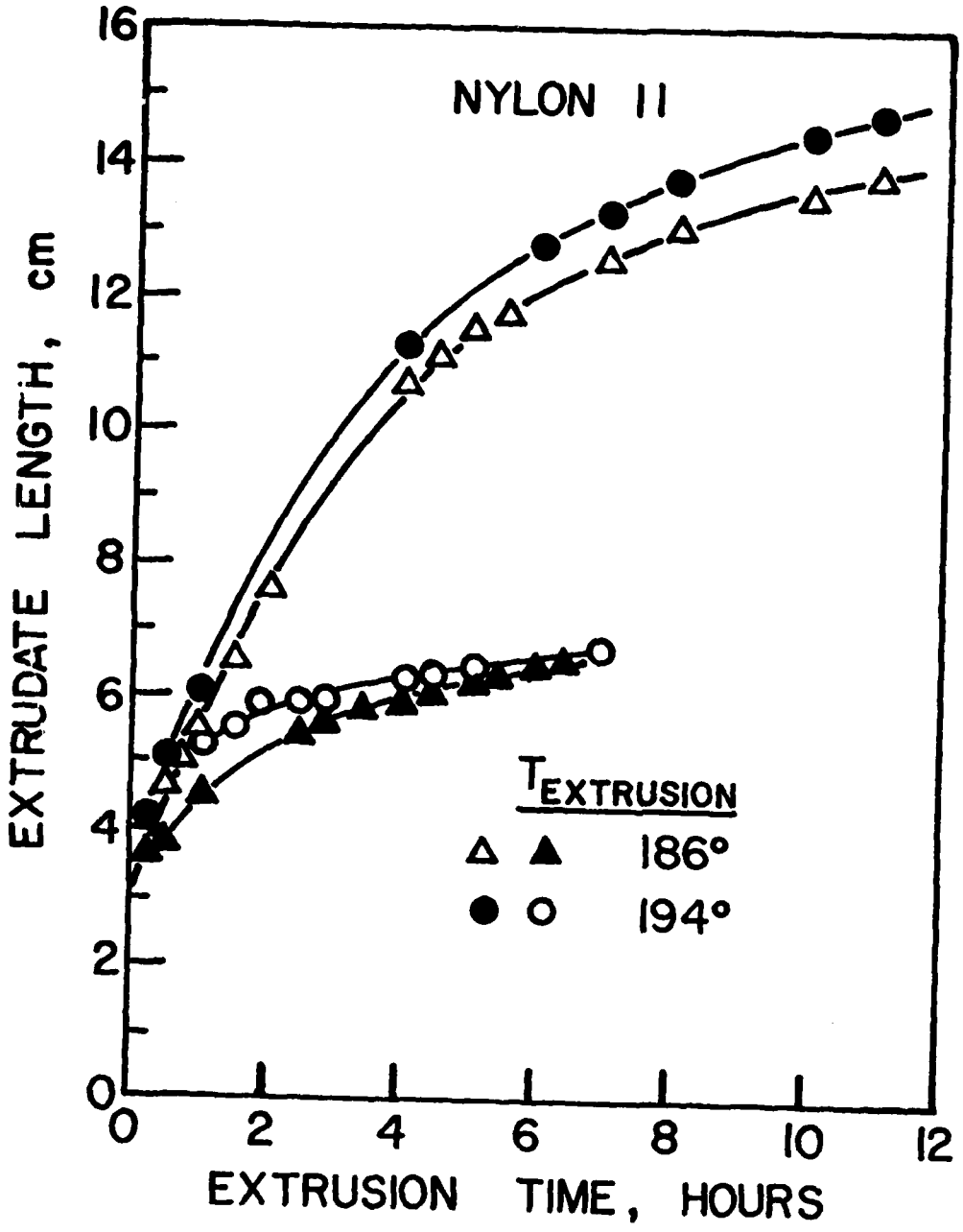
NYLON 11
EXTRUDATE LENGTH, cm
EXTRUSION TIME, HOURS
0
2
4
6
8
10
12
14
16
T EXTRUSION
186°
194°

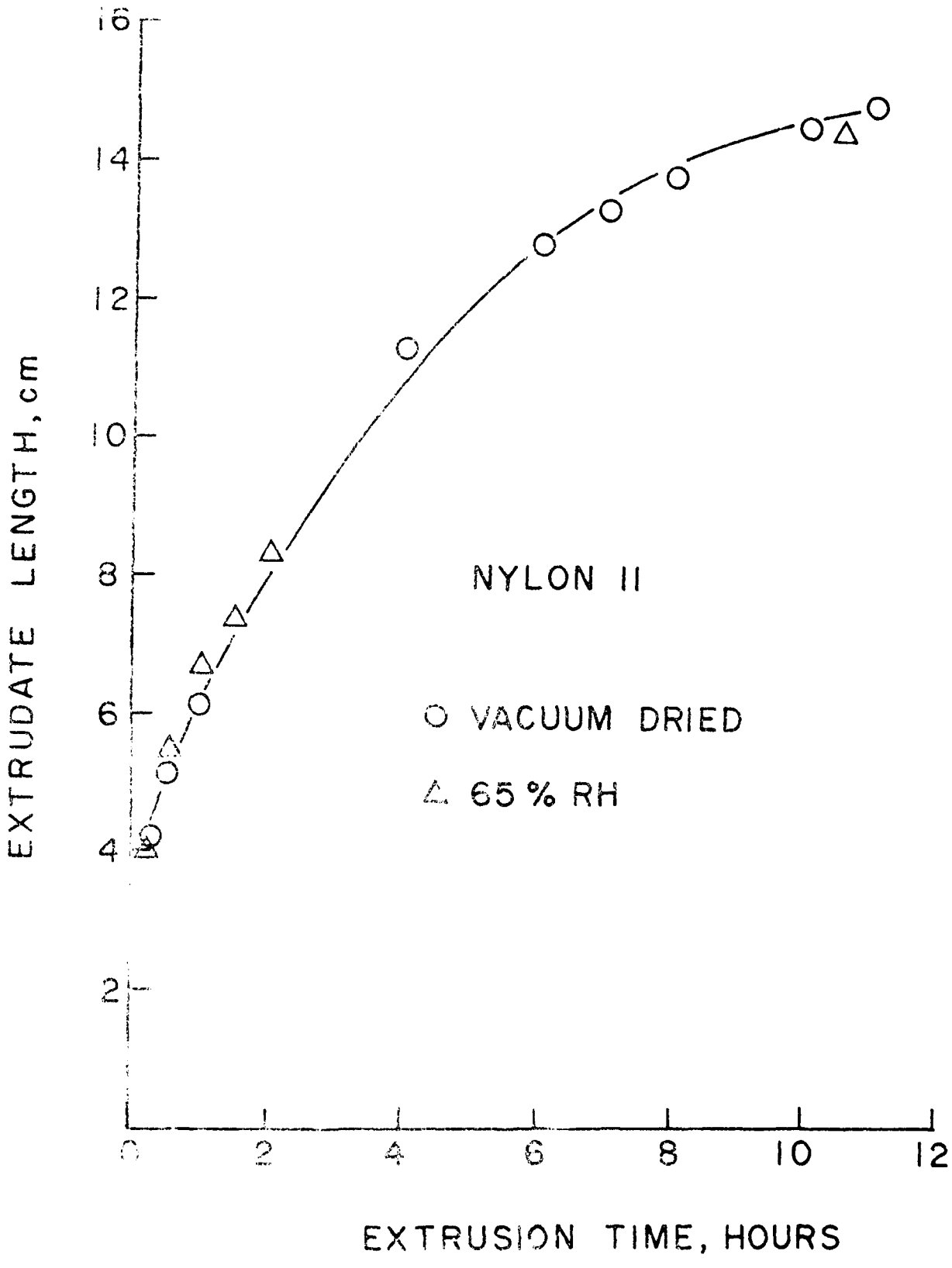
EXTRUDATE LENGTH, cm
16
14
12
10
8
6
4
2
0
2
4
6
8
10
12
EXTRUSION TIME, HOURS
NYLON 11
VACUUM DRIED
65 % RH

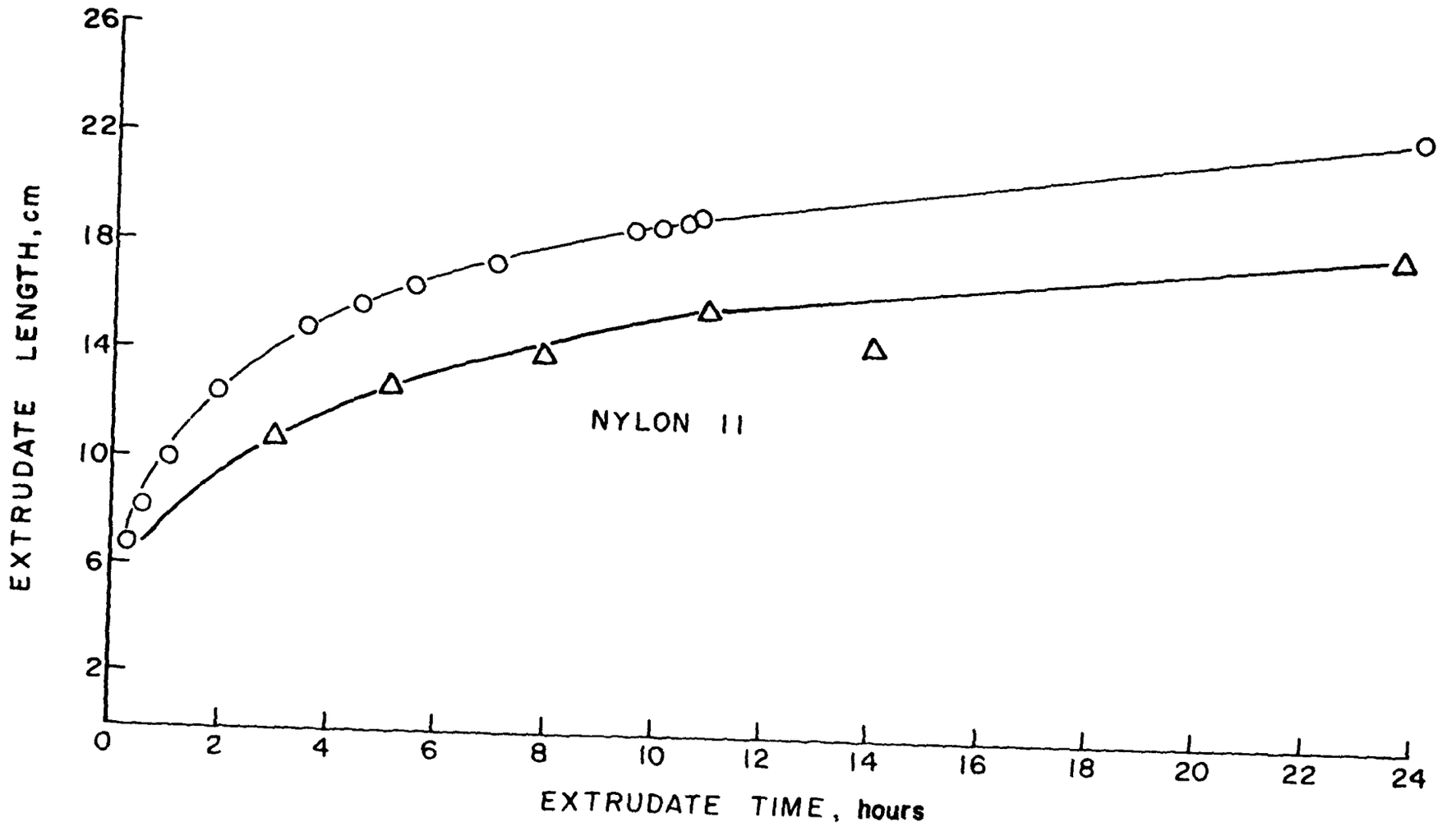
EXTRUDATE LENGTH, cm
26
22
18
14
10
6
2
NYLON 11
0
2
4
6
8
10
12
14
16
18
20
22
24
EXTRUDATE TIME, hours

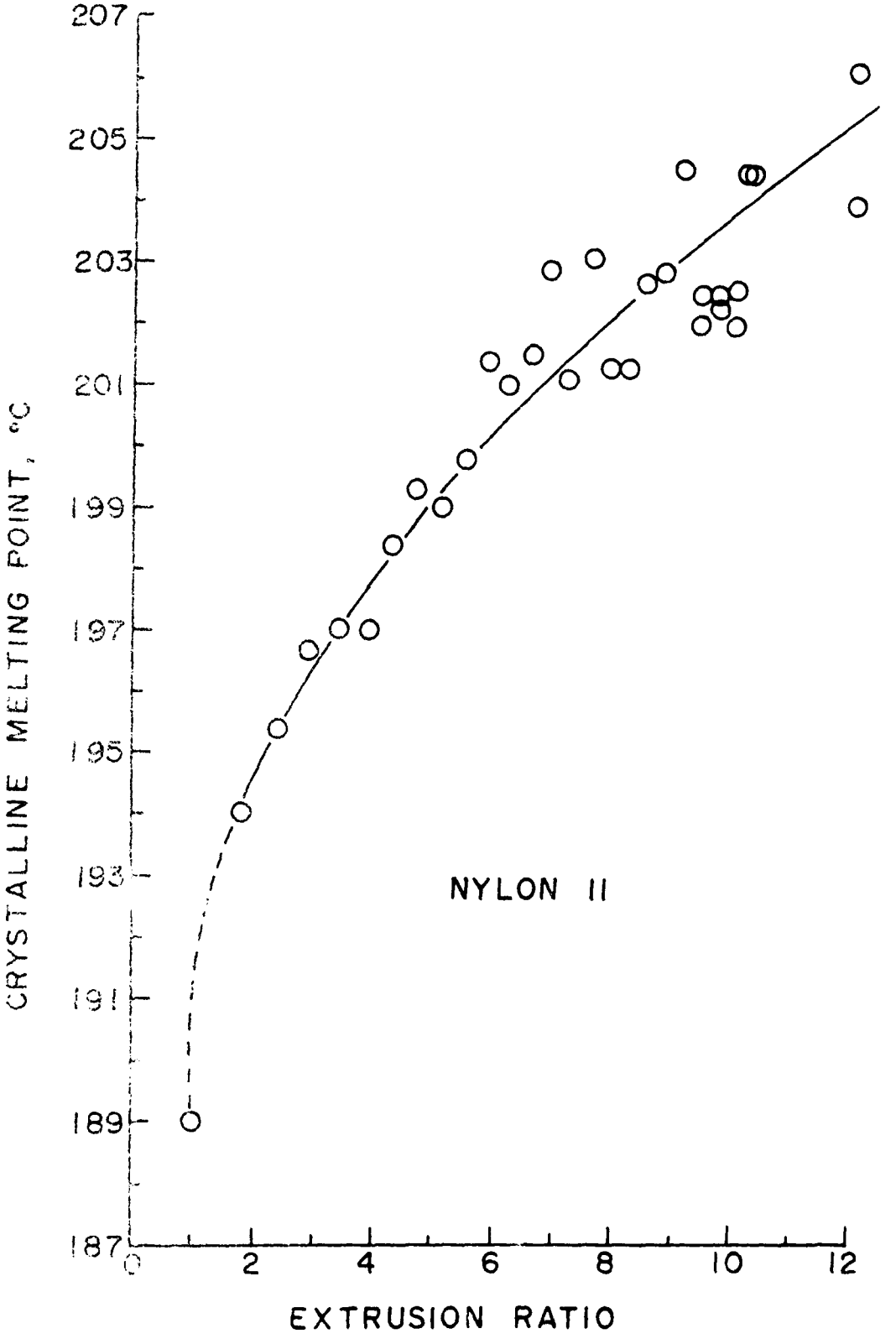
207
205
203
201
199
197
195
193
191
189
187
0
2
4
6
8
10
12
CRYSTALLINE MELTING POINT, °C
EXTRUSION RATIO
NYLON 11

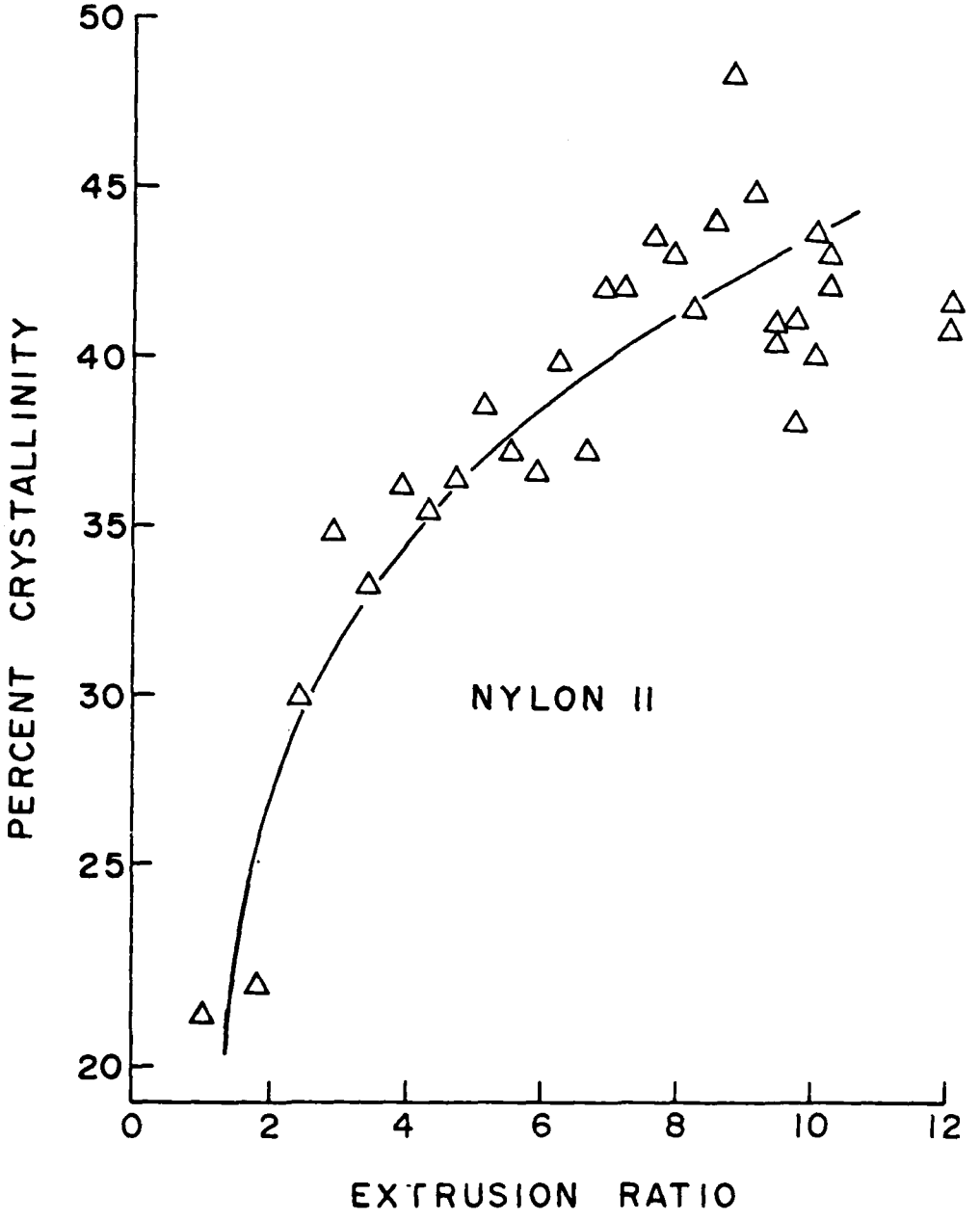
50
45
40
35
30
25
20
PERCENT CRYSTALLINITY
NYLON 11
0
2
4
6
8
10
12
EXTRUSION RATIO

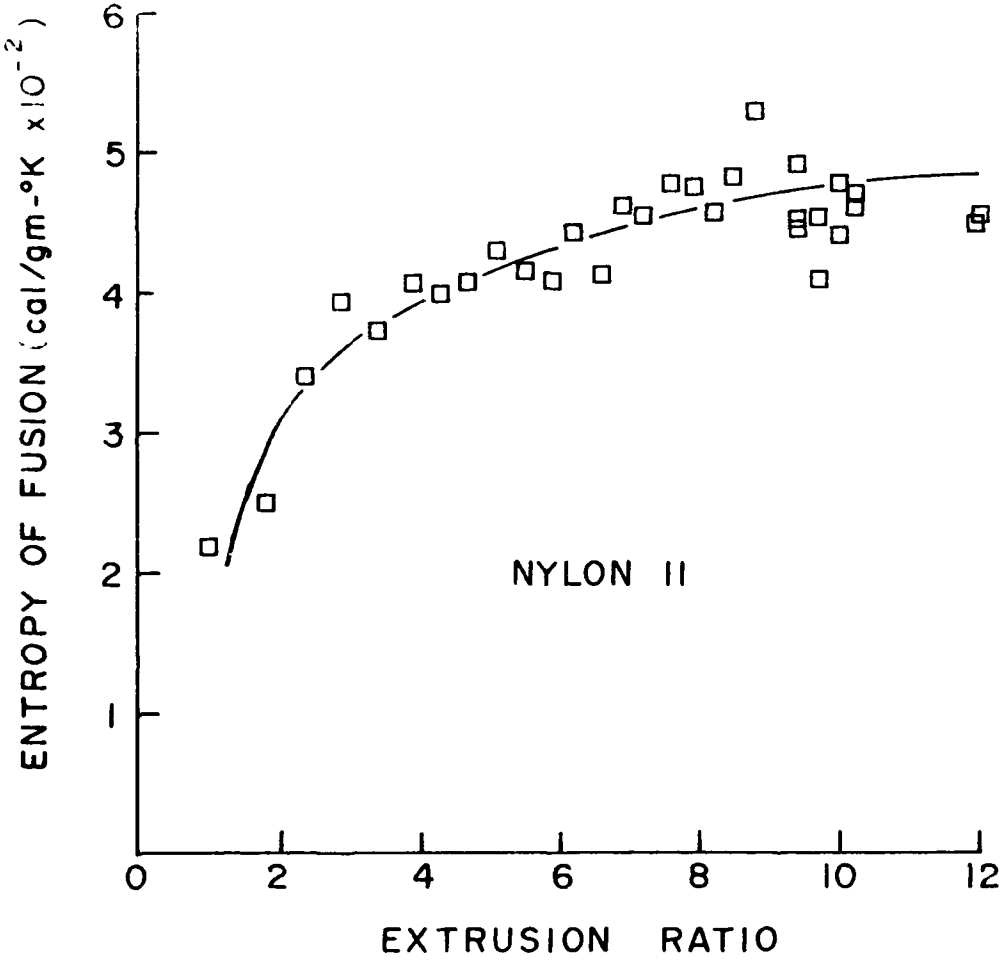
ENTROPY OF FUSION (cal/gm-°K x10⁻²)
6
5
4
3
2
1
0
2
4
6
8
10
12
EXTRUSION RATIO
NYLON 11

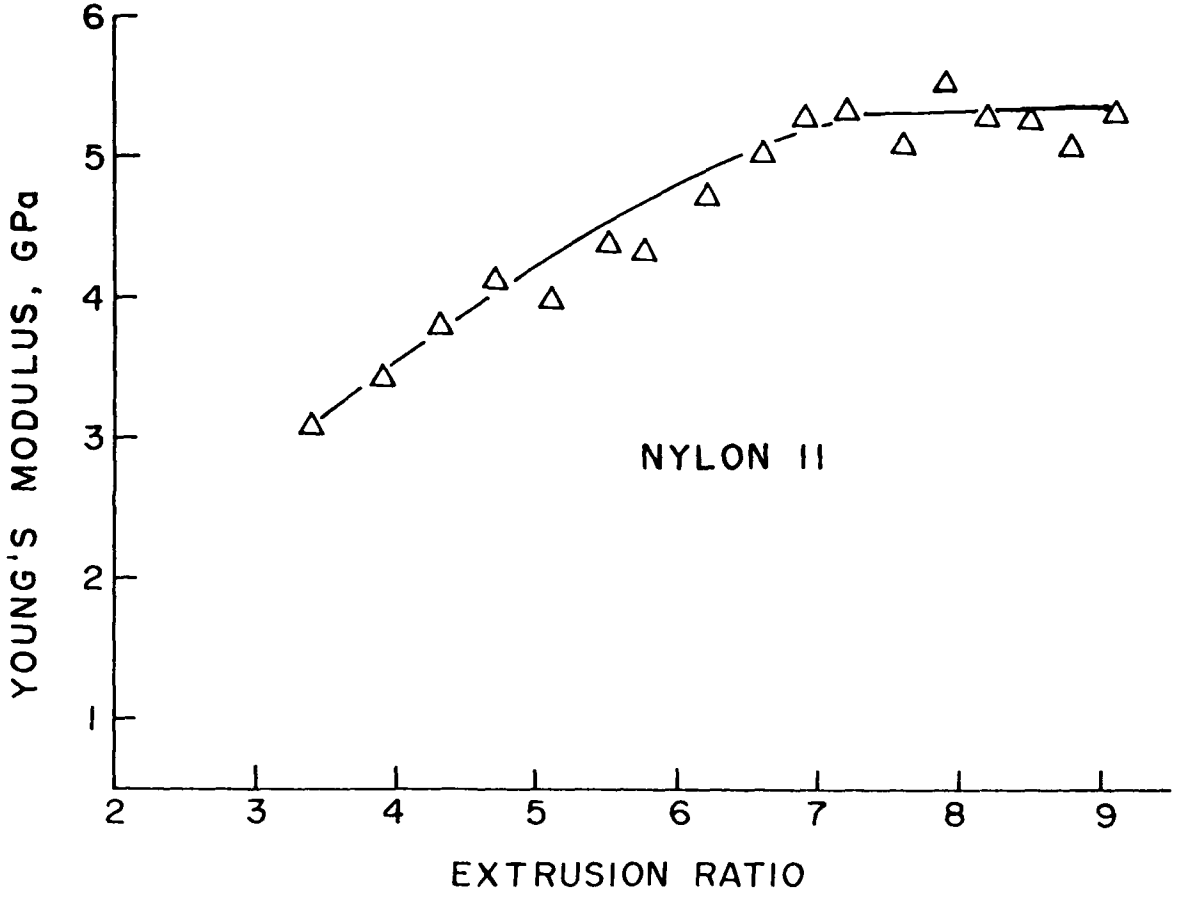
YOUNG'S MODULUS, GPa
6
5
4
3
2
1
NYLON 11
2
3
4
5
6
7
8
9
EXTRUSION RATIO

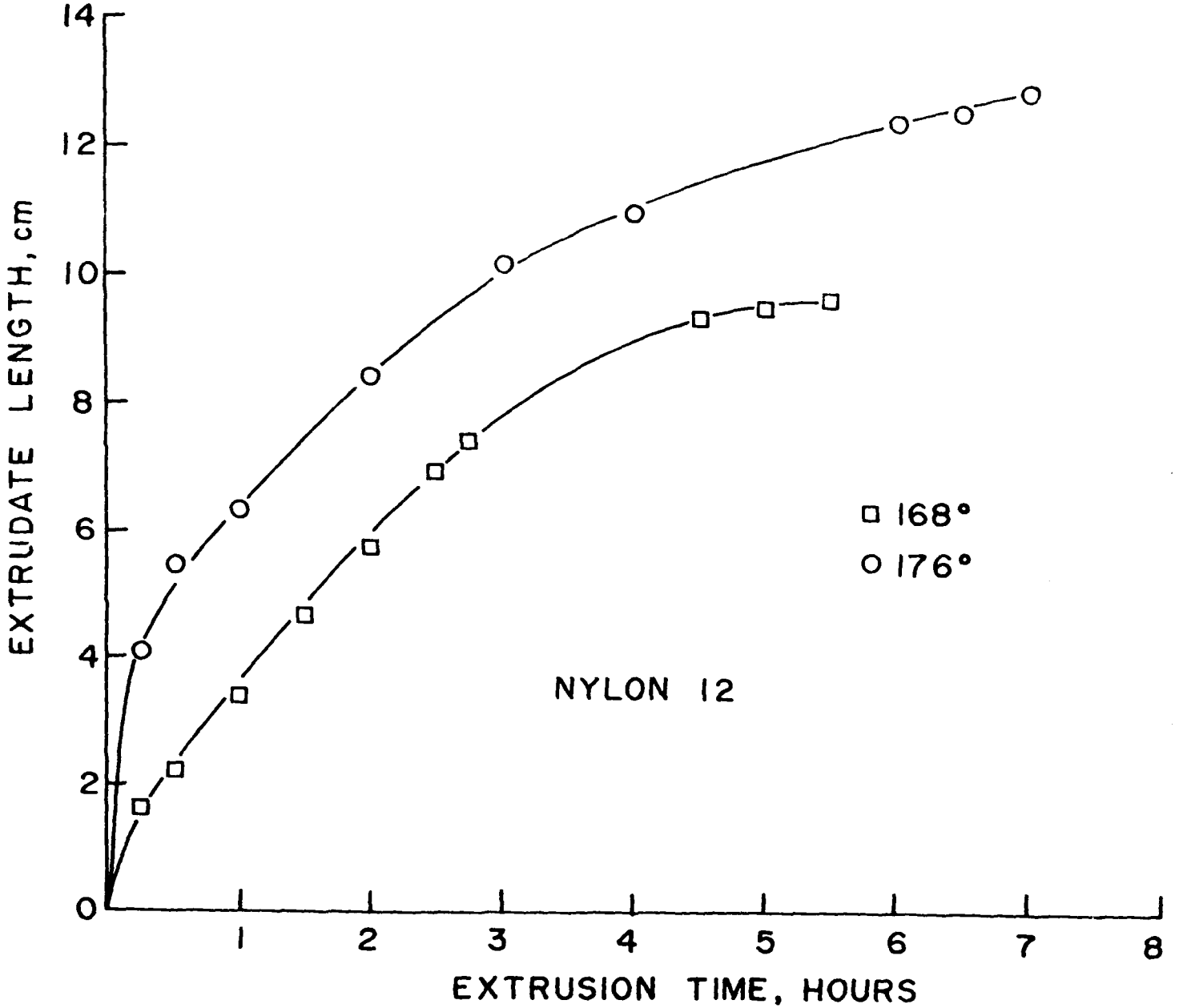
EXTRUDATE LENGTH, cm
EXTRUSION TIME, HOURS
NYLON 12
□ 168°
○ 176°
0
2
4
6
8
10
12
14
1
2
3
4
5
6
7
8

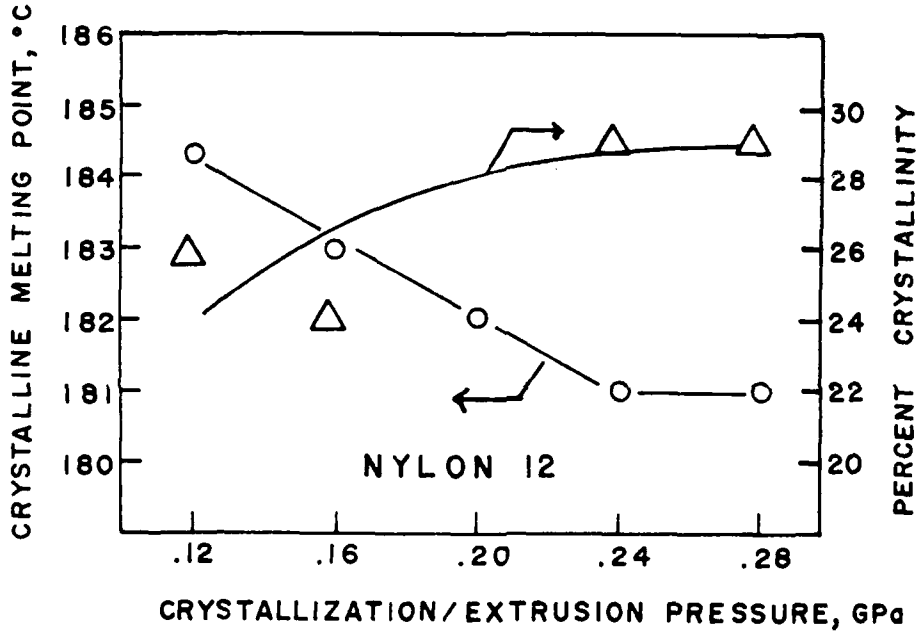
CRYSTALLINE MELTING POINT, °C
186
185
184
183
182
181
180
30
28
26
24
22
20
PERCENT CRYSTALLINITY
NYLON 12
.12
.16
.20
.24
.28
CRYSTALLIZATION/EXTRUSION PRESSURE, GPa

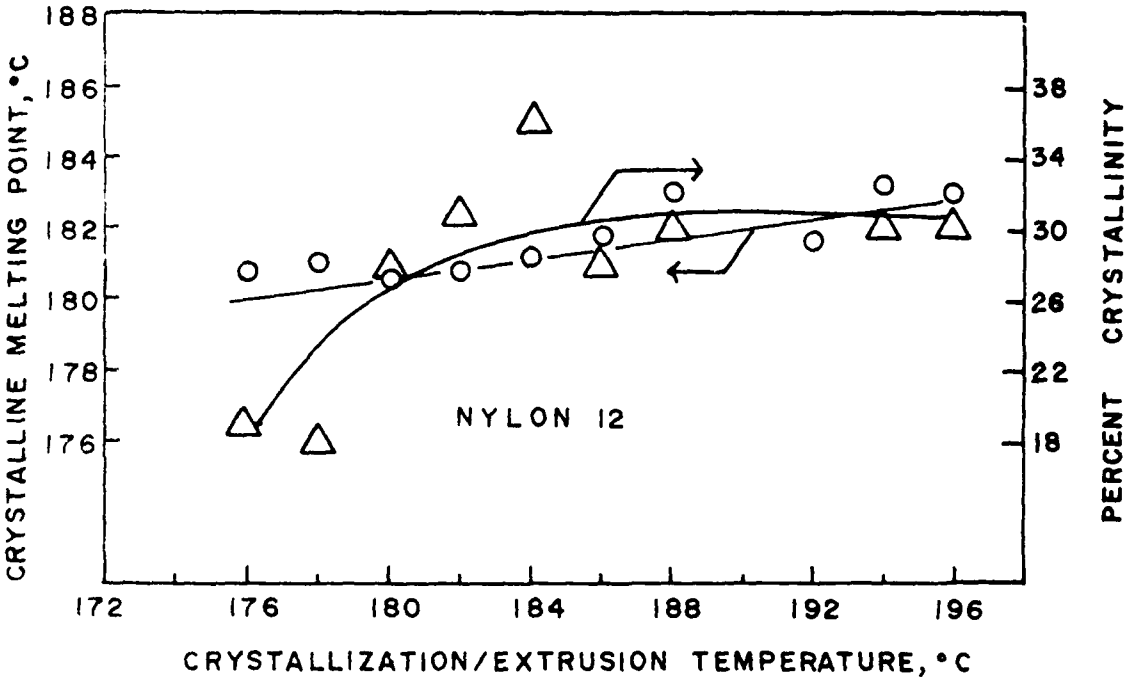
188
186
184
182
180
178
176
CRYSTALLINE MELTING POINT, °C
38
34
30
26
22
18
PERCENT CRYSTALLINITY
NYLON 12
172
176
180
184
188
192
196
CRYSTALLIZATION/EXTRUSION TEMPERATURE, °C

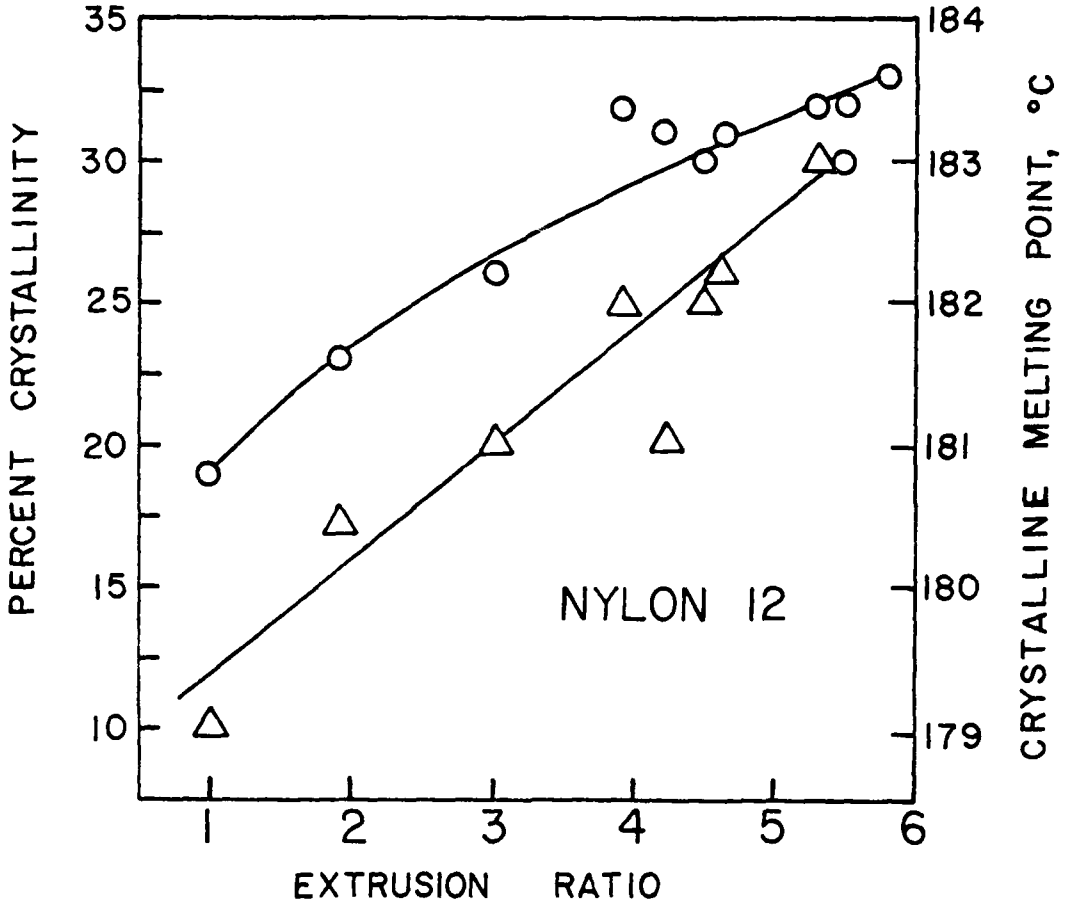
PERCENT CRYSTALLINITY
35
30
25
20
15
10
184
183
182
181
180
179
CRYSTALLINE MELTING POINT, °C
NYLON 12
1
2
3
4
5
6
EXTRUSION RATIO

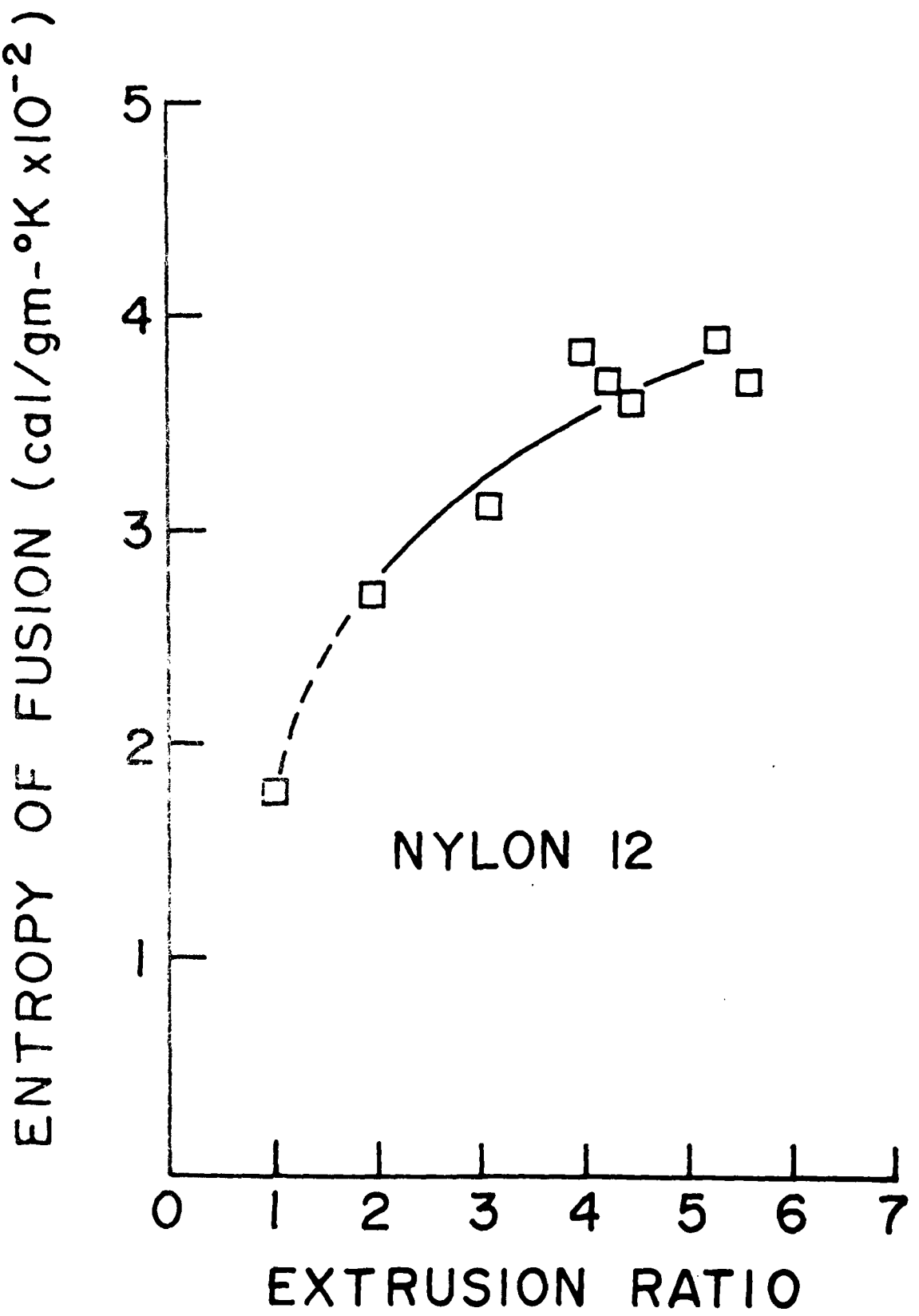
ENTROPY OF FUSION (cal/gm-°K x10⁻²)
5
4
3
2
1
NYLON 12
0
1
2
3
4
5
6
7
EXTRUSION RATIO

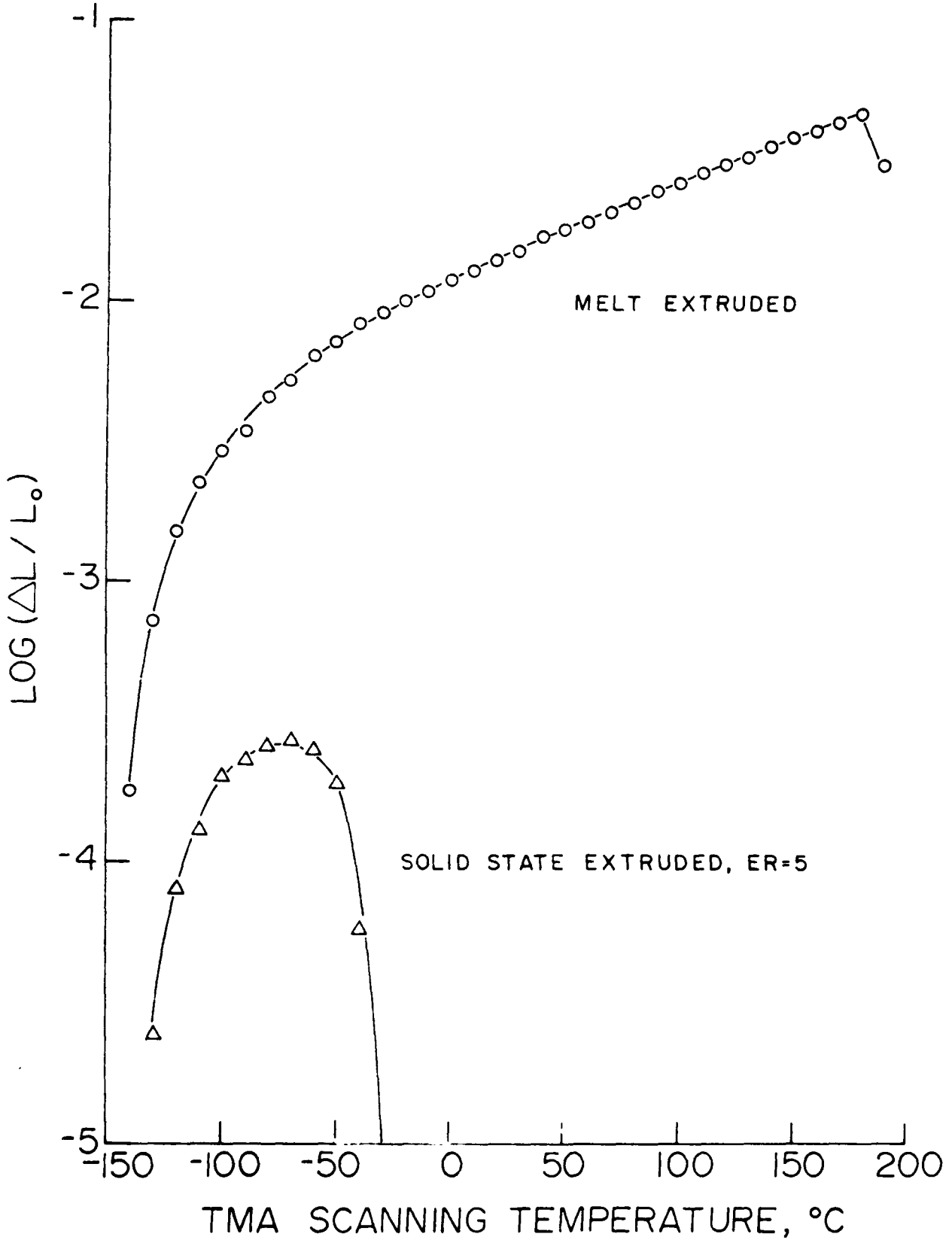
-1
-2
-3
-4
-5
LOG (ΔL / L₀)
MELT EXTRUDED
SOLID STATE EXTRUDED, ER=5
-150
-100
-50
0
50
100
150
200
TMA SCANNING TEMPERATURE, °C

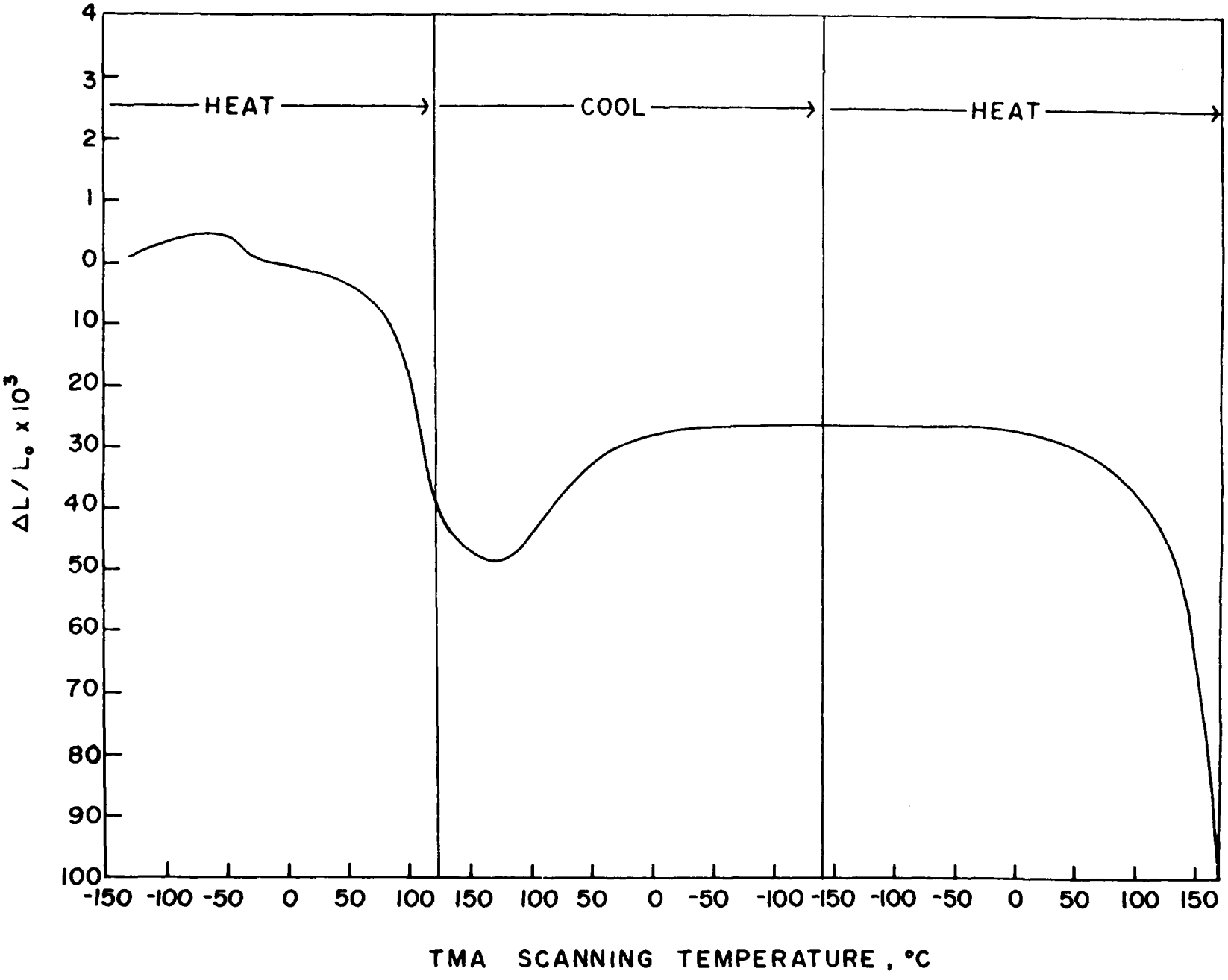
HEAT
COOL
HEAT
4
3
2
1
0
10
20
30
40
50
60
70
80
90
100
ΔL / L₀ x 10³
-150 -100 -50 0 50 100 150 100 50 0 -50 -100 -150 -100 -50 0 50 100 150
TMA SCANNING TEMPERATURE, °C

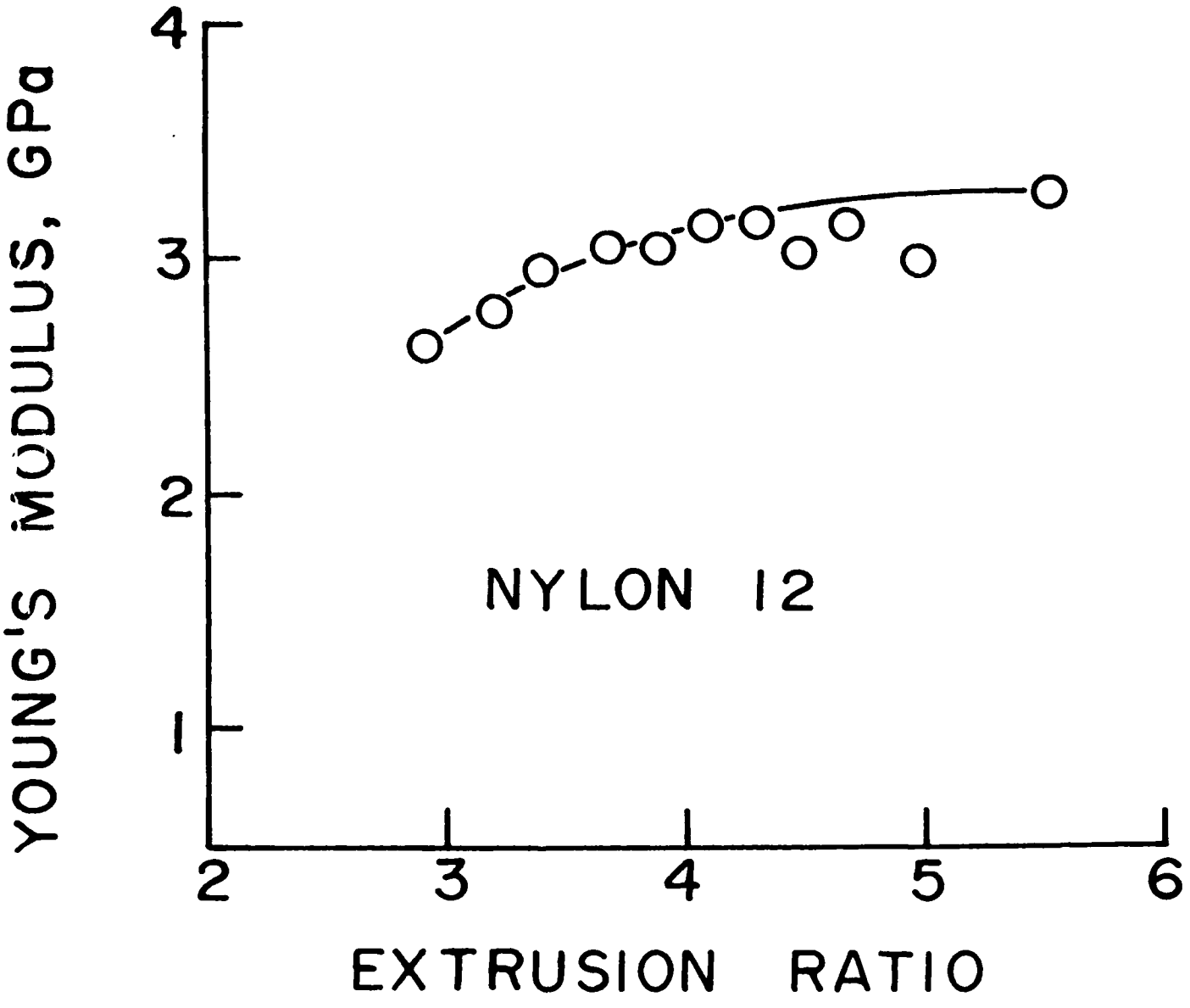
YOUNG'S MODULUS, GPa
4
3
2
1
NYLON 12
2
3
4
5
6
EXTRUSION RATIO

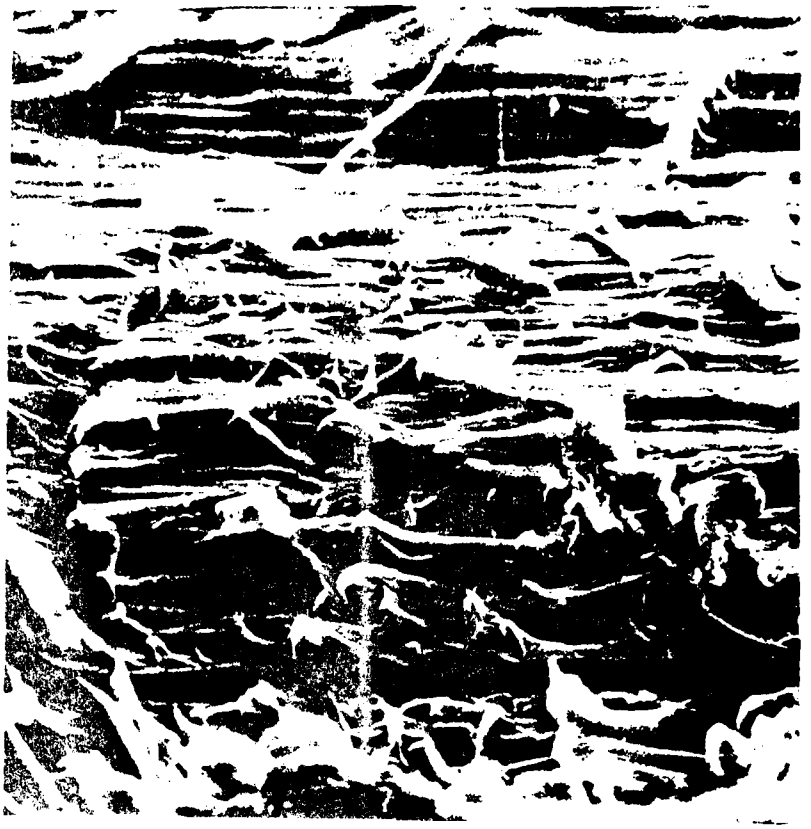

a.
10μ

b.
10μ

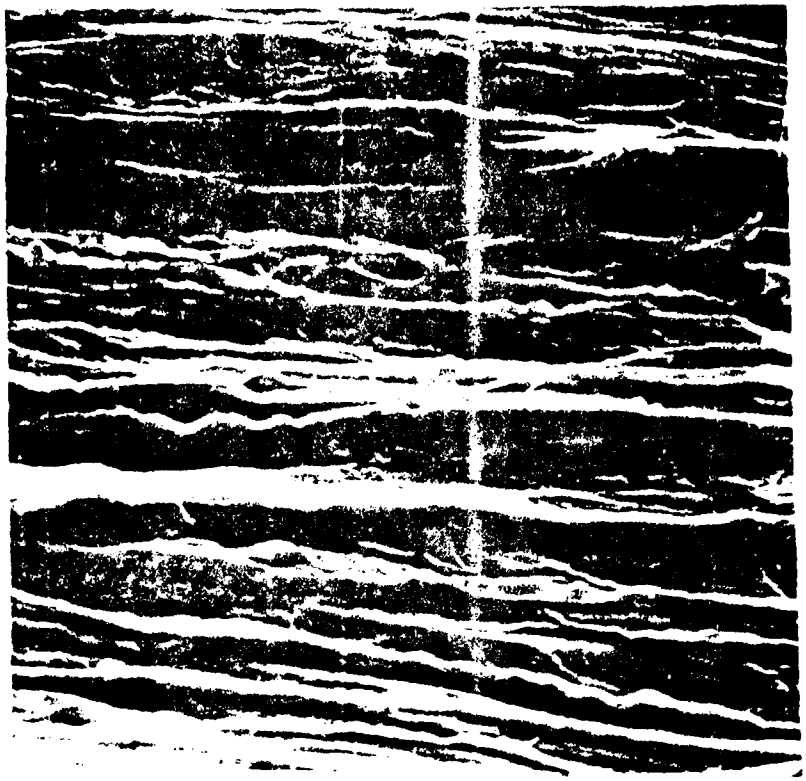

a.

1μ

b.

1μ

Unclassified

SECURITY CLASSIFICATION OF THIS PAGE (When Data Entered)

REPORT DOCUMENTATION PAGE		READ INSTRUCTIONS BEFORE COMPLETING FORM
1. REPORT NUMBER Technical Report No. 12	2. GOVT ACCESSION NO.	3. RECIPIENT'S CATALOG NUMBER
4. TITLE (and Subtitle) Solid State Extrusion of Nylons 11 and 12; Processing, Morphology and Properties		5. TYPE OF REPORT & PERIOD COVERED Interim 6. PERFORMING ORG. REPORT NUMBER
7. AUTHOR(s) William G. Perkins and Roger S. Porter		8. CONTRACT OR GRANT NUMBER(s) N00014-75-C-0686
9. PERFORMING ORGANIZATION NAME AND ADDRESS Polymer Science and Engineering University of Massachusetts Amherst, Massachusetts 01003		10. PROGRAM ELEMENT, PROJECT, TASK AREA & WORK UNIT NUMBERS NR 356-581
11. CONTROLLING OFFICE NAME AND ADDRESS ONR Branch Office 666 Summer Street Boston, Massachusetts 02210		12. REPORT DATE December 14, 1979 13. NUMBER OF PAGES 45 (incl. tables and figures)
14. MONITORING AGENCY NAME & ADDRESS(if different from Controlling Office)		15. SECURITY CLASS. (of this report) Unclassified 15a. DECLASSIFICATION/DOWNGRADING SCHEDULE

16. DISTRIBUTION STATEMENT (of this Report)

Approved for public release; distribution unlimited

17. DISTRIBUTION STATEMENT (of the abstract entered in Block 20, if different from Report)

18. SUPPLEMENTARY NOTES

19. KEY WORDS (Continue on reverse side if necessary and identify by block number)

nylon-11, nylon-12, extrusion, moisture, morphology, modulus, pressure, processing

20. ABSTRACT (Continue on reverse side if necessary and identify by block number)

Monofilaments of poly(11-amino-undecanoic acid) (nylon 11) and poly-(laurylactam) (nylon 12) have been produced via solid state extrusion in an Instron capillary rheometer. The resulting morphology plus physical and mechanical properties were investigated. For nylon 11, crystalline melting point (Tm) increased 16°C at an extrusion ratio (ER) of 12, over the undrawn material, while percent crystallinity (Xc) was up 23%. Nylon 12, extruded to a maximum ER of 6, realized an increase in Tm of 4°C at ER=5 and an Xc increase of 14%. Young's modulus for nylon 11

DD FORM 1 JAN 73 1473 EDITION OF 1 NOV 65 IS OBSOLETE
S/N 0102-014-6601

Unclassified

SECURITY CLASSIFICATION OF THIS PAGE (When Data Entered)

increased from 3 GPa at an ER≤3 to 5.5 GPa at an ER≤7, then levelled off at higher draw. For nylon 12, the value climbed from 2.5 at ER≤3 to ≤ 3.3 GPa at ER≤5.5. Conventionally melt-spun and cold-drawn nylon 11 fibers exhibit a Young's modulus of 2.7 GPa; nylon 12 fibers, 2.9 GPa. Atmospheric moisture loss was found not to affect solid state extrusion of these higher nylons. Increases in extrusion temperature and/or pressure increased extrusion rate. The flow activation energy of nylon 11 was 73 Kcal/mole at 0.24 GPa extrusion pressure, and 124 Kcal/mole at 0.49 GPa. Calculated apparent viscosities were ~ 10^{14} poise and ~ 10^{15} poise, respectively. The morphologies were shown by electron microscopy to be microfibrillar and the resulting monofilaments were transparent to visible light.

P4-2/A23

472:GAN:716:tam
78u472-608

TECHNICAL REPORT DISTRIBUTION LIST, GEN

	No. Copies
Office of Naval Research Attn: Code 472 800 North Quincy Street Arlington, Virginia 22217	2
ONR Branch Office Attn: Dr. George Sandoz 536 S. Clark Street Chicago, Illinois 60605	1
ONR Branch Office Attn: Scientific Dept. 715 Broadway New York, New York 10003	1
ONR Branch Office 1030 East Green Street Pasadena, California 91106	1
ONR Branch Office Attn: Dr. L. H. Peebles Building 114, Section D 666 Summer Street Boston, Massachusetts 02210	1
Director, Naval Research Laboratory Attn: Code 6100 Washington, D.C. 20390	1
The Assistant Secretary of the Navy (R,E&S) Department of the Navy Room 4E736, Pentagon Washington, D.C. 20350	1
Commander, Naval Air Systems Command Attn: Code 310C (H. Rosenwasser) Department of the Navy Washington, D.C. 20360	1
Defense Documentation Center Building 5, Cameron Station Alexandria, Virginia 22314	12
Dr. Fred Saalfeld Chemistry Division Naval Research Laboratory Washington, D.C. 20375	1
U.S. Army Research Office Attn: CRD-AA-IP P.O. Box 1211 Research Triangle Park, N.C. 27709	1
Naval Ocean Systems Center Attn: Mr. Joe McCartney San Diego, California 92152	1
Naval Weapons Center Attn: Dr. A. B. Amster, Chemistry Division China Lake, California 93555	1
Naval Civil Engineering Laboratory Attn: Dr. R. W. Drisko Port Hueneme, California 93401	1
Department of Physics & Chemistry Naval Postgraduate School Monterey, California 93940	1
Dr. A. L. Slafkosky Scientific Advisor Commandant of the Marine Corps (Code RD-1) Washington, D.C. 20380	1
Office of Naval Research Attn: Dr. Richard S. Miller 800 N. Quincy Street Arlington, Virginia 22217	1
Naval Ship Research and Development Center Attn: Dr. G. Bosmajian, Applied Chemistry Division Annapolis, Maryland 21401	1
Naval Ocean Systems Center Attn: Dr. S. Yamamoto, Marine Sciences Division San Diego, California 91232	1
Mr. John Boyle Materials Branch Naval Ship Engineering Center Philadelphia, Pennsylvania 19112	1

472:GAN:716:tam
78u472-608

TECHNICAL REPORT DISTRIBUTION LIST, GEN

	No. Copies
Dr. Rudolph J. Marcus Office of Naval Research Scientific Liaison Group American Embassy APO San Francisco 96503	1
Mr. James Kelley DTNSRDC Code 2803 Annapolis, Maryland 21402	1

472:GAN:716:abc
78u472-608

TECHNICAL REPORT DISTRIBUTION LIST, 356A

	No. Copies
Dr. Stephen H. Carr Department of Materials Science Northwestern University Evanston, Illinois 60201	1
Dr. M. Broadhurst Bulk Properties Section National Bureau of Standards U.S. Department of Commerce Washington, D.C. 20234	2
Dr. T. A. Litovitz Department of Physics Catholic University of America Washington, D.C. 20017	1
Professor G. Whitesides Department of Chemistry Massachusetts Institute of Technology Cambridge, Massachusetts 02139	1
Professor J. Wang Department of Chemistry University of Utah Salt Lake City, Utah 84112	1
Dr. V. Stannett Department of Chemical Engineering North Carolina State University Raleigh, North Carolina 27607	1
Dr. D. R. Uhlmann Department of Metallurgy and Material Science Massachusetts Institute of Technology Cambridge, Massachusetts 02139	1
Naval Surface Weapons Center White Oak Silver Spring, Maryland 20910 Attn: Dr. J. M. Augl Dr. B. Hartman	1
Dr. G. Goodman Globe Union Incorporated 5757 North Green Bay Avenue Milwaukee, Wisconsin 53201	1
Picatinny Arsenal SMUPA-FR-M-D Dover, New Jersey 07801 Attn: A. M. Anzalone Building 3401	1
Dr. J. K. Gillham Princeton University Department of Chemistry Princeton, New Jersey 08540	1
Douglas Aircraft Co. 3855 Lakewood Boulevard Long Beach, California 90846 Attn: Technical Library Cl 290/36-84 AUTO-Sutton	1
Dr. E. Baer Department of Macromolecular Science Case Western Reserve University Cleveland, Ohio 44106	1
Dr. K. D. Pae Department of Mechanics and Materials Science Rutgers University New Brunswick, New Jersey 08903	1
NASA-Lewis Research Center 21000 Brookpark Road Cleveland, Ohio 44135 Attn: Dr. T. T. Serofini, MS-49-1	1
Dr. Charles H. Sherman, Code TD 121 Naval Underwater Systems Center New London, Connecticut	1
Dr. William Risen Department of Chemistry Brown University Providence, Rhode Island 02192	1
Dr. Alan Gent Department of Physics University of Akron Akron, Ohio 44304	1

TECHNICAL REPORT DISTRIBUTION LIST, 356A

	No. Copies
Mr. Robert W. Jones Advanced Projects Manager Hughes Aircraft Company Mail Station D 132 Culver City, California 90230	1
Dr. C. Giori IIT Research Institute 10 West 35 Street Chicago, Illinois 60616	1
Dr. M. Litt Department of Macromolecular Science Case Western Reserve University Cleveland, Ohio 44106	1
Dr. R. S. Roe Department of of Materials Science and Metallurgical Engineering University of Cincinnati Cincinnati, Ohio 45221	1
Dr. Robert E. Cohen Chemical Engineering Department Massachusetts Institute of Technology Cambridge, Massachusetts 02139	1
Dr. David Roylance Department of Materials Science and Engineering Massachusetts Institute of Technology Cambridge, Massachusetts 02039	1
Dr. T. P. Conlon, Jr., Code 3622 Sandia Laboratories Sandia Corporation Albuquerque, New Mexico	1
Dr. Martin Kaufmann, Head Materials Research Branch, Code 4542 Naval Weapons Center China Lake, California 93555	1
Professor S. Senturia Department of Electrical Engineering Massachusetts Institute of Technology Cambridge, Massachusetts 02139	1
Dr. T. J. Reinhart, Jr., Chief Composite and Fibrous Materials Branch Nonmetallic Materials Division Department of the Air Force Air Force Materials Laboratory (AFSC) Wright-Patterson Air Force Base, Ohio 4543	1
Dr. J. Lando Department of Macromolecular Science Case Western Reserve University Cleveland, Ohio 44106	
Dr. J. White Chemical and Metallurgical Engineering University of Tennessee Knoxville, Tennessee 37916	
Dr. J. A. Manson Materials Research Center Lehigh University Bethlehem, Pennsylvania 18015	1
Dr. R. F. Helmreich Contract RD&E Dow Chemical Co. Midland, Michigan 48640	1
Dr. R. S. Porter University of Massachusetts Department of Polymer Science and Engineering Amherst, Massachusetts 01002	1
Professor Garth Wilkes Department of Chemical Engineering Virginia Polytechnic Institute and State University Blacksburg, Virginia 24061	1
Dr. Kurt Baum Fluorochem Inc. 6233 North Irwindale Avenue Azuza, California 91702	1
Professor C. S. Paik Sung Department of Materials Sciences and Engineering Room 8-109 Massachusetts Institute of Technology Cambridge, Massachusetts 02139	1